NPL
National Physical Laboratory

FRM4SST-CRICR-NPL-002_ISSUE-1

Fiducial Reference Measurements for Sea Surface Temperature (FRM4SST)

D90 - Result from CEOS International Thermal Infrared Radiometer Inter-comparison (CRIC)
Part 2 of 3: Laboratory Comparison of Radiometers

Yoshiro Yamada, NPL
Subrena Harris, NPL
Michael Hayes, NPL
Rob Simpson, NPL
Werenfrid Wimmer, Univ. of Southampton
Raymond Holmes, Univ. of Southampton
Tim Nightingale, STFC Rutherford Appleton Laboratory
Arrow Lee, STFC Rutherford Appleton Laboratory
Nis Jepsen, Danish Meteorological Institute
Nicole Morgan, CSIRO / Australian Bureau of Meteorology
Frank-M. Göttsche, Karlsruhe Institute of Technology
Raquel Niclòs, Univ. of Valencia
Martín Perelló, Univ. of Valencia
Craig Donlon, European Space Agency
Nigel Fox, NPL

March 2023

INTENTIONALLY BLANK

Fiducial Reference Measurements for Sea Surface Temperature
(FRM4SST)

D90 – Results from CEOS International Thermal Infrared Radiometer
Inter-comparison (CRIC)
Part 2 of 3: Laboratory Comparison of Radiometers

Yoshiro Yamada, Subrena Harris, Michael Hayes, Rob Simpson,
Werenfrid Wimmer, Raymond Holmes, Tim Nightingale, Arrow Lee, Nis
Jepsen, Nicole Morgan, Frank-M. Göttsche, Raquel Niclòs, Martín
Perelló, Craig Donlon & Nigel Fox

National Physical Laboratory
Hampton Road, Teddington, Middlesex, TW11 0LW

Approved on behalf of NPLML by
Martin Dury, Science Area Leader.

DOCUMENT MANAGEMENT

Issue	Revision	Date of Issue/revision	Description of Changes
1	1	19/01/2023	Creation of document (Draft A)
	2	30/03/2023	Draft B

DOCUMENT APPROVAL

Contractor Approval

Name	Role in Project	Signature & Date (dd/mm/yyyy)	
Y Yamada	Metrology lead and comparison pilot	*Y.Y.*	30/03/2023
N Fox	Metrology lead and CEOS WGCV rep	*Nigel Fox*	30/03/2023

CUSTOMER APPROVAL

Name	Role in Project	Signature	Date (dd/mm/yyyy)
C Donlon	ESA Technical Officer		

APPLICABLE DOCUMENTS

AD Ref.	Ver. /Iss.	Title
AD-1	Issue – 1	Fiducial Reference Measurements for Sea Surface Temperature (FRM4SST): Protocol for FRM4SST CRIC Laboratory Comparison of Radiometers and Blackbodies
AD-2	Issue – 1	Fiducial Reference Measurements for Sea Surface Temperature (FRM4SST): Protocol for FRM4SST CRIC Field Comparison of Radiometers
AD-3	Issue – 2	Fiducial Reference Measurements for Sea Surface Temperature (FRM4SST): D80 - Implementation plan for Laboratory and Field Comparisons of Radiometers and Blackbodies
AD-4	Issue – 1	Fiducial Reference Measurements for Sea Surface Temperature (FRM4SST): D90 – Results from CEOS International Thermal Infrared Radiometer Inter-comparison (CRIC) Part 1 of 3: Laboratory Comparison of Blackbodies
AD-5	Issue – 1	Fiducial Reference Measurements for Sea Surface Temperature (FRM4SST): D90 – Results from CEOS International Thermal Infrared Radiometer Inter-comparison (CRIC) Part 3 of 3: Field Comparison of Radiometers

CONTENTS

ACRONYMS AND ABBREVIATIONS

CEOS	Committee on Earth Observation Satellites
IR	Infra-Red
NPL	National Physical Laboratory
SST	Sea Surface Temperature
WGCV	Working Group for Calibration and Validation
BB	Blackbody
NH3-BB	Ammonia heatpipe Blackbody
SL-BB	Stirred Liquid bath Blackbody
RSS	Root Sum Square
SPRT	Standard Platinum Resistance Thermometer
CRV	Comparison Reference Value
SI	International System of Units
ITS-90	International Temperature Standards of 1990

1   INTRODUCTION

The measurement of the Earth's surface temperature is a critical product for meteorology and an essential parameter/indicator for climate monitoring. Satellites have been monitoring global surface temperature for some time, and have established sufficient consistency and accuracy between in-flight sensors to claim that it is of "climate quality". However, it is essential that such measurements are fully anchored to International System of Units (SI) and that there is a direct regular correlation with "true" surface/in-situ based measurements.

The most accurate of these surface-based measurements (used for validation) are derived from field-deployed IR radiometers. These are in principle calibrated traceably to SI, generally through a reference radiance blackbody (BB). Such instrumentation is of varying design, operated by different teams in different parts of the globe. It is essential for the integrity of their use, to provide validation data for satellites in-flight and to provide the link to future sensors, that any differences in the results obtained between them are understood. This knowledge will allow any potential biases to be removed and not transferred to satellite sensors. This knowledge can only be determined through formal comparison of the instrumentation, both in terms of its measurement capabilities in relation to primary "laboratory based" calibration facilities, and its use in the field. The provision of a fully traceable link to SI as part of this process ensures that the data are evidentially robust and can claim their status as a "climate data record".

The "satellite IR Cal/Val community" is well versed in the need and value of such comparisons having held highly successful exercises in Miami in 2001 [1, 2], and at the National Physical Laboratory (NPL), Teddington UK, in 2009 [3, 4] and in 2016 [5, 6, 7, 8], all carried out under the auspices of CEOS. However, six years had passed since the last comparison and it was considered timely to repeat/update the process, and so a similar comparison was repeated in 2022. The 2022 comparison included:

  a. Comparison of the BB reference standards used for calibrating the radiometers (laboratory based).
  b. Comparison of the radiometer response to a common SI-traceable BB target (laboratory based).
  c. Evaluation of differences in radiometer response when viewing sea surface targets in particular the effects of external environmental conditions such as sky brightness (field-based).

The comparison took place during two weeks in June of 2022. The first week involved the laboratory-based comparisons (a. b.) at NPL. The second week was devoted to the field-based comparison (c.), at the tip of Boscombe Pier in Bournemouth, UK. Unlike the previous comparison in 2016, land surface temperature measurement was not a part of the 2022 comparison. Details of all the comparisons including the comparison scheme can be found in the protocols of the comparisons [AD-1, AD-2] and the implementation plan [AD-3].

This is Part 2 of a three-part report, and covers the result of the laboratory comparison of the radiometers of the participants against the NPL reference BBs. Reports on the laboratory comparison of the participant BBs carried out at NPL can be found in Part 1 [AD-4], and the field comparison of radiometers at Boscombe Pier in Part 3 [AD-5].

2 ORGANISATION OF THE COMPARISON

2.1 PILOT

As in the recent previous comparisons, NPL, the UK National Metrology Institute (NMI), served as pilot for the 2022 comparison. NPL, as the pilot, was responsible for inviting participants, for preparing the protocols that the participants have agreed, for providing the implementation plan to enable participants to prepare for the comparison, for providing the reference source traceable to the SI for comparison, for the analysis of data following appropriate processing by individual participants and for the compilation of a report that is agreed by all participants.

2.2 PARTICIPANTS

A call was made inviting potential participants in the related scientific community to express their interest to participate in December 2021. The list of participants that actually participated is shown in Table 1. As can be seen, seven participants including the pilot took part. This is a reduction from the previous 2016 comparison where eleven institutes, including the pilot, were present. Although there was a certain number of expressed interests, no institute could participate from the USA and China, primarily due to travel restrictions imposed due to the COVID-19 pandemic.

Table 1. Comparison participants

Contact person	Short version	Institute
Yoshiro Yamada (pilot)	NPL	National Physical Laboratory Hampton Road, Teddington, Middlesex, TW11 0LW, United Kingdom
Werenfrid Wimmer	UoS	University of Southampton European Way, Southampton, SO19 9TX, United Kingdom
Tim Nightingale	RAL	STFC Rutherford Appleton Laboratory Harwell Campus, Didcot,Oxon OX11 0QX United Kingdom
Nis Jepsen	DMI	Danish Meteorological Institute Lyngbyvej 100, 2100 Copenhagen Ø, Denmark
Nicole Morgan	CSIRO	CSIRO / Australian Bureau of Meteorology CSIRO, 3-4 Castray Esplanade, Battery Point, TAS 7150 Australia
Frank-M. Göttsche	KIT	IMK-ASF / Karlsruhe Institute of Technology Hermann-von-Helmholtz-Platz 1, 76344 Eggenstein-Leopoldshafen, Germany
Raquel Niclòs	UoV	Dept. of Earth Physics and Thermodynamics, University of Valencia 50 Dr. Moliner. ES-46100, Burjassot (Valencia), Spain

3 TIMELINE

The preparation for the comparison, the comparison measurements, and the analysis and report writing were conducted according to the timeline shown in Table 2. The laboratory comparison was undertaken in the week 13 – 17 June 2022, before the week of the field comparison at Boscombe Pier.

Table 2. Comparison activity timeline

Invitation to participate	December 2021
Formal agreement of protocol	May 2022
Participants send preliminary report of measurement system and uncertainty to pilot	May 2022
Laboratory measurement of participants' radiometers against reference BBs. Laboratory measurement of participants' BBs by reference thermometer.	13 – 17 June 2022
SST measurement comparison of participants' radiometers.	20 – 24 June 2022
Participants send all data and reports to pilot	~ August 2022
Pre-Draft A result communication with individual participants for comments, corrections and confirmation	~ November 2022
Draft A report circulation among participants (tentative)	January 2023

4   COMPARISON SCHEME

4.1   OVERVIEW OF THE COMPARISON

The laboratory comparison exercise was conducted by having the participants' artifacts gathered in a laboratory at NPL and one by one compared with an SI-traceable reference standard of NPL. The measurand to be compared was the brightness temperature of the BBs at approximately 10 μm, in the range from −30 °C to 50 °C. For this, a laboratory large enough to accommodate all participant radiometers and BBs, as well as the NPL reference radiometer and BBs, was prepared.

The radiometer comparison consisted of measurement of the NPL standard variable-temperature BBs by the participants' infrared radiometers. Each participant measured either one or two of the NPL BBs dependent on their radiometer's operating range. The variable temperature BBs, operated by the pilot, have reference standard platinum resistance thermometers (SPRTs) measuring the cavity temperature (which will remain unknown to the participants) and a well-defined emissivity. The SPRTs are calibrated traceable to the International Temperature Scale of 1990 (ITS-90) [9].
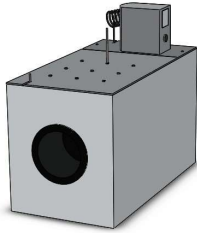
4.2   REFERENCE STANDARDS

Two variable temperature BBs were utilised in this comparison. One is an ammonia heatpipe blackbody (NH3-BB), and the other is a stirred liquid bath blackbody (SL-BB). The comparison reference values (CRVs) are given by the SPRTs which are calibrated traceable to the NPL primary temperature standards, measuring the temperature of the BBs. Of the two, the NH3-BB was the same as the one used in the previous comparison [6,8]. In the current comparison, a second blackbody source (SL-BB) was introduced, so that the two measurements can be run side by side and covering different temperature ranges for improved efficiency.

The specifications for the two NPL variable temperature BBs are shown in Table 3 below. Details are described in [10, 11]. In recent years the uncertainty for the NH3-BB has been re-evaluated and is slightly increased from what is shown in [10], now being in the range from 0.13 K to 0.10 K below 0 °C and 0.095 K above 20 °C (k = 2). The SL-BB has a smaller uncertainty, which is around 0.05 K at 0 °C to 30 °C (k = 2).

Both BBs have purge systems utilising a flow of dry nitrogen gas which is applied below 10 °C. They also have detachable apertures which have been applied during the comparison measurements at set-point temperatures below the dew point to prevent ambient air from entering the cavity that can cause condensation of dew and frost. When the aperture is removed at around room temperature, the decrease in emissivity and the increase in the cavity reflectance of the ambient radiation almost completely cancel each other, so the same correction and uncertainty have been applied for with and without the aperture.

Table 3 Variable-temperature blackbody specifications

	Ammonia heatpipe BB (NH3-BB)	Stirred liquid bath BB (SL-BB)
Aperture diameter	ɸ 75 mm max	ɸ 160 mm max
Aperture distance from front panel	75 mm	35 mm
Emissivity	0.9993@10 µm	0.9998 @11 µm*
Temperature range	−40 °C – 50 °C	−10 °C – 40 °C
Reference thermometer	PRT	PRT
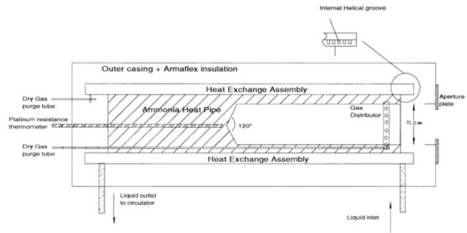
*: With ɸ 80 mm aperture applied to the cavity opening

A view of the laboratory is shown in Fig. 1. On the left, the CSIRO Sea surface temperature Autonomous Radiometer (ISAR) radiometer is measuring the SL-BB. On the right, the UoV CIMEL radiometer is being set up to measure the NH3-BB.
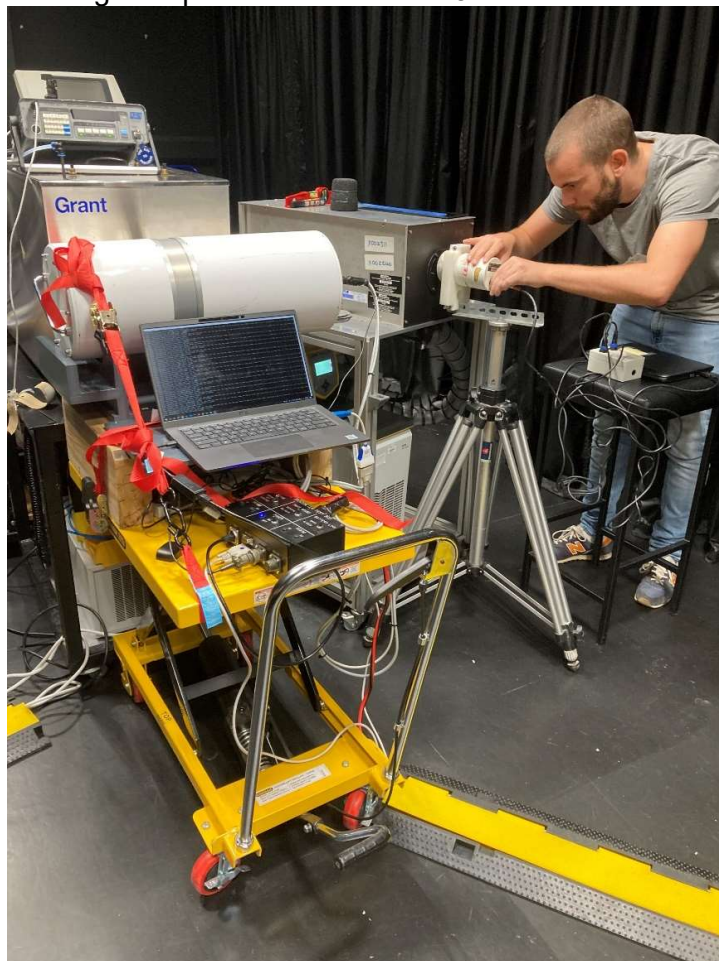
Figure 1 Radiometers measuring the reference BBs

4.3   MEASUREMENT TEMPERATURES

The NPL BBs were set at the nominal temperatures covering the range from −30 °C to 50 °C as shown in Table 4. All participants participated in all temperature points except for 50 °C, for which only UoV, KIT and RAL participated. However, CSIRO later withdrew from submitting their results for three of the points after noticing an issue with the alignment of their radiometer against the NH3-BB. The temperature range of main interest for SST measurement is 10 °C to 30 °C, so the SL-BB, having better temperature stability and higher emissivity as well as larger aperture for ease in alignment, was assigned to cover this range. The NH3-BB, being able to rapidly change set-point temperature and covering a wider range, was assigned to cover the higher and lower ends. At 0 °C and 30 °C, both BBs were measured so that a check could be made of the agreement of the radiometer measurements made with the two BBs.

Table 4   Measurement temperature points

Reference source	Nominal temperature / °C
Ammonia heatpipe BB (NH3-BB)	−30, −15, 0, 30, 35, 40, 50
Stirred liquid bath BB (SL-BB)	0, 10, 20, 30

4.4   MEASURAND

The principle measurand in the comparison is brightness temperature at 10 μm. Temperature here refers to that of the ITS-90.

5   PARTICIPANTS' RADIOMETERS AND MEASUREMENTS

In the following, descriptions of the participants' radiometers are given, as reported by each participant, and measured data for the reference blackbody brightness temperatures are shown for each participant. The error bars are the standard uncertainties claimed by each participant combined with measurement uncertainty evaluated, where possible, from the uncertainty of the mean of repeated measurements. The reference values, defined in the protocol as the brightness temperatures of the reference BBs declared by NPL (i.e. the temperatures given by the SPRTs within the source, corrected for emissivity and ambient reflection), are also plotted, with their standard uncertainties shown as error bars. All date and time values are given in British Summer Time (BST).

5.1   MEASUREMENT BY UoV

5.1.1   Description of radiometer, route of traceability and uncertainty contributions

Make and type of the Radiometer: CIMEL Electronique CE312-2, six spectral bands (two units)

Outline Technical description of instrument: Type of detector: thermopile, operating at ambient temperature. Six spectral bands: B1 8.0 μm-13.3 μm, B2 10.9 μm-11.7 μm, B3 10.2 μm-11.0 μm, B4 9.0 μm-9.3 μm, B5 8.5 μm-8.9 μm, and B6 8.3 μm-8.6 μm. Broad band: germanium window and zinc sulphide filters. Narrow bands: interference filters. Field of view: 10º. The instrument has a built-in radiance reference made of a concealable gold-coated mirror which enables comparison between the target radiance and the reference radiation from inside the detector cavity. The temperature of the detector is measured with a calibrated platinum resistance thermometer (PRT), thus allowing compensation for the cavity radiation. The relevant outputs of the radiometer are the detector temperature and the difference in digital counts between the signals from the target and the detector cavity. For detail see [12,13,14].

Establishment or traceability route for primary calibration including date of last realisation and breakdown of uncertainty: The following error analysis is based on

laboratory measurements with the Landcal blackbody P80P (combined standard uncertainty of 0.34 K; [AD-4, AD-5]) on May, 2022, and estimates from the above references. Blackbody measurements were taken at eleven fixed temperatures (from 0 ºC to 50 ºC) in two different runs with instrument realigning. The values reported below are typical values for all blackbody temperatures considered for each band of each radiometer (units 1 and 2). The mean values considering all bands of each radiometer are also given.

Type A

Table 5 Repeatability: Typical value of the standard deviation of 15 measurements at fixed blackbody temperature without re-alignment of radiometer.

Unit 1	B1	B2	B3	B4	B5	B6	mean
K	0.012	0.05	0.04	0.06	0.07	0.09	0.05
% (at 300 K)	0.004	0.015	0.014	0.02	0.02	0.03	0.018

Unit 2	B1	B2	B3	B4	B5	B6	mean
K	0.014	0.03	0.03	0.04	0.04	0.05	0.03
% (at 300 K)	0.005	0.009	0.009	0.013	0.014	0.017	0.011

Table 6 Reproducibility: Typical value of difference between two runs of radiometer measurements at the same blackbody temperature including re-alignment.

Unit 1	B1	B2	B3	B4	B5	B6	mean
K	0.06	0.05	0.05	0.07	0.07	0.07	0.06
% (at 300 K)	0.02	0.017	0.018	0.02	0.02	0.02	0.02

Unit 2	B1	B2	B3	B4	B5	B6	mean
K	0.04	0.03	0.04	0.09	0.06	0.07	0.06
% (at 300 K)	0.014	0.011	0.012	0.03	0.019	0.03	0.019

Table 7 Total Type A uncertainty (RSS):

Unit 1	B1	B2	B3	B4	B5	B6	mean
K	0.06	0.07	0.07	0.09	0.10	0.11	0.08
% (at 300 K)	0.02	0.02	0.02	0.03	0.03	0.04	0.03

Unit 2	B1	B2	B3	B4	B5	B6	mean
K	0.04	0.04	0.05	0.10	0.07	0.09	0.06
% (at 300 K)	0.015	0.015	0.015	0.03	0.02	0.03	0.02

Type B

- Primary calibration: 0.34 K (estimation of the combined standard uncertainty of the Landcal blackbody P80P).
- Linearity of radiometer: 0.06 K (Typical value for all bands in the temperature range 0 ºC – 40 ºC according to [12]).
- Drift since calibration: It has been corrected for using the calibration measurements performed with the Landcal blackbody P80P mentioned above. A linear correcting equation has been derived for each band and radiometer, with the radiometer measured temperature and the detector temperature as inputs. The uncertainty for this correction is the root sum square (RSS) of the typical estimation uncertainty of the linear regression (0.06 K for unit 1 and 0.05 K for unit 2) and the uncertainties resulting

from the propagation of input temperature errors (standard deviations for 15 measurement at a fixed temperature) in the linear correcting equation. The resulting uncertainty in the correction of calibration drift is 0.08 K for unit 1 and 0.06 K for unit 2.

- Ambient temperature fluctuations: The effect of ambient temperature fluctuations is compensated by the CE312 radiometers by measuring the detector cavity temperature by means of a calibrated PRT. The uncertainty in this process is the uncertainty of the internal PRT, which is 0.04 K according to [13].
- Atmospheric absorption/emission: Negligible (< 0.01K) due to very short path length and radiometers working in the atmospheric window.

Total Type B standard uncertainty (RSS): 0.36 K for unit 1 and 0.35 K for unit 2.

Type A + Type B standard uncertainty (RSS) (k = 1): 0.37 K for unit 1 and 0.36 K for unit 2. (See Tables 8 and 9.)

Table 8 Uncertainty Contributions associated with UoV CE312-2 Unit 1

Uncertainty Contribution	Type A Uncertainty in Value / K / % [1]	Type B Uncertainty in Value / K	Standard uncertainty in Brightness temperature / K
Repeatability of measurement	0.05 K / 0.018 %		0.05
Reproducibility of measurement	0.06 K / 0.02%		0.06
Primary calibration Linearity of radiometer		0.34	0.34
		0.06	0.06
Drift since calibration		0.08	0.08
		0.04	0.04
Ambient temperature fluctuations			
Atmospheric absorption/emission			
Combined uncertainty (RSS)	0.08 K / 0.03 %	0.36	0.37

[1] at 300 K   Note: All uncertainty values are in standard uncertainties (i.e. k = 1)

Table 9 Uncertainty Contributions associated with UoV CE312-2 Unit 2

Uncertainty Contribution	Type A Uncertainty in Value / K / % [1]	Type B Uncertainty in Value / K	Standard uncertainty in Brightness temperature / K
Repeatability of measurement	0.03 K / 0.011 %		0.03
Reproducibility of measurement	0.06 K / 0.019 %		0.06
Primary calibration Linearity of radiometer		0.34	0.34
Drift since calibration		0.06	0.06
		0.06	0.06
Ambient temperature fluctuations		0.04	0.04
Atmospheric absorption/emission			
Combined uncertainty (RSS)	0.06 K / 0.02 %	0.35	0.36

[1] at 300 K   Note: All uncertainty values are in standard uncertainties (i.e. $k = 1$)

Operational methodology during measurement campaign: The Landcal Blackbody Source P80P was set at eleven fixed temperatures (0-50 ºC) in two different runs. Enough time was allowed for the blackbody to reach equilibrium at each temperature. Radiometers were aligned with the blackbody cavity, and placed at a distance so that the field of view was smaller than the cavity diameter. Standard processing (see [12,13,14]) was applied to the radiometer readouts to calculate the equivalent brightness temperature. Due to the radiometer responsivity drift with time, a correction is applied depending on the difference between the measured brightness temperature (T_m) and the detector temperature (T_d) (details in [14]):

$T_c = T_m + a(T_m - T_d) + b$

where T_c is the corrected or re-calibrated brightness temperature, and *a* and *b* are band-dependent coefficients derived from linear regression from the calibration measurements at the eleven temperatures in the two runs.

Radiometer usage (deployment), previous use of instrument and planned applications: Mainly, field measurements of land surface temperature and emissivity for validation of thermal infrared products from satellite sensors, but also measurements of SST and inland water surface temperature in the framework of specific campaigns.

5.1.2   Measured data

Figures 2 and 3 show the measurement results reported by UoV for the SL-BB and for the NH3-BB, respectively. Two radiometers, each with six spectral bands are used. The twelve plots correspond to measurement with these bands.
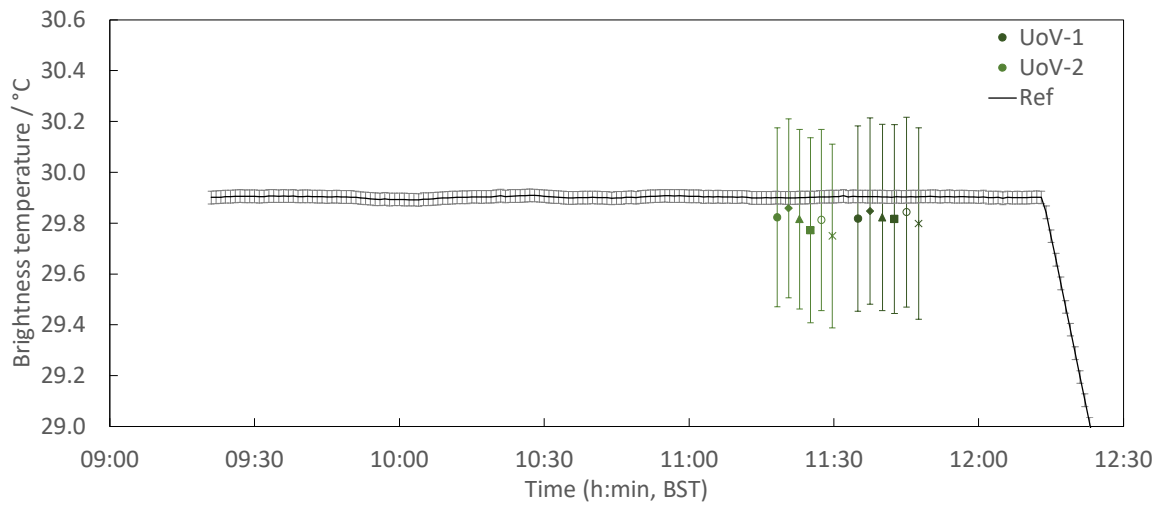
a) 30 °C (16 June 2022)
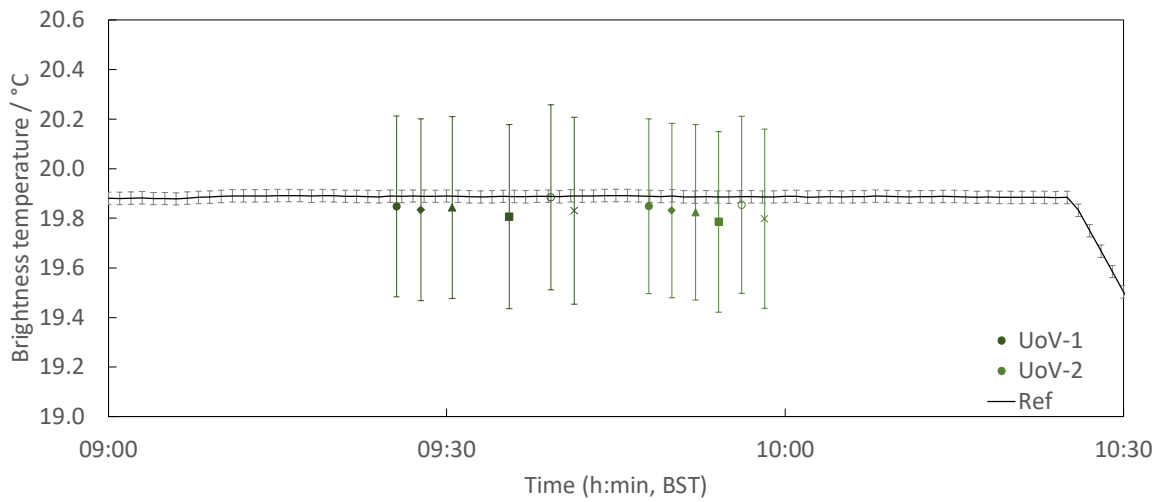
b) 20 °C (14 June 2022)
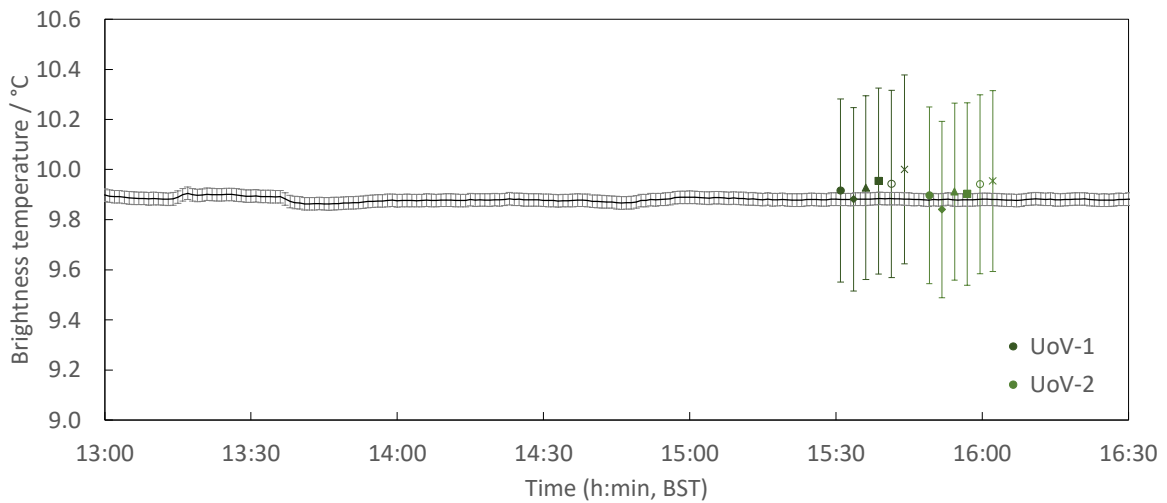
c) 10 °C (14 June 2022)

Figure 2 SL-BB measurement by UoV (Error bar denotes standard uncertainty) (continued on next page)
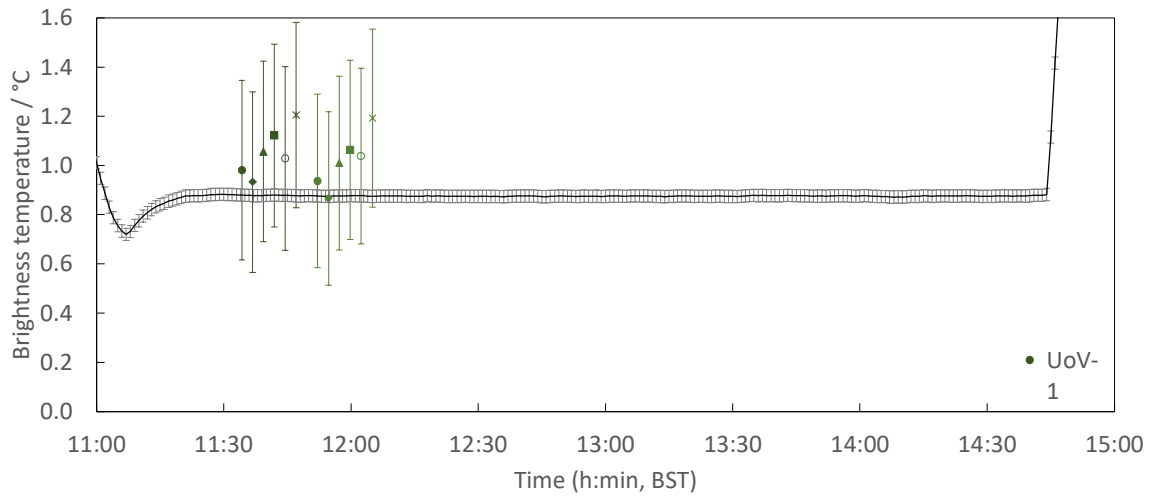
d) 0 °C (15 June 2022)
Figure 2 SL-BB measurement by UoV (Error bar denotes standard uncertainty) (cont.)
For both UoV-1 and UoV-2 radiometers, each plot corresponds to a spectral band, from B1
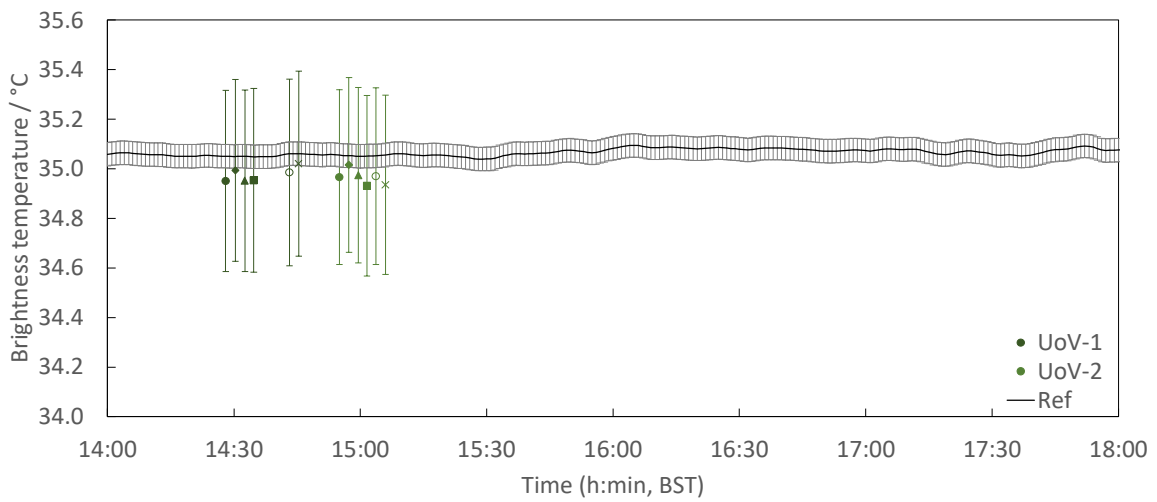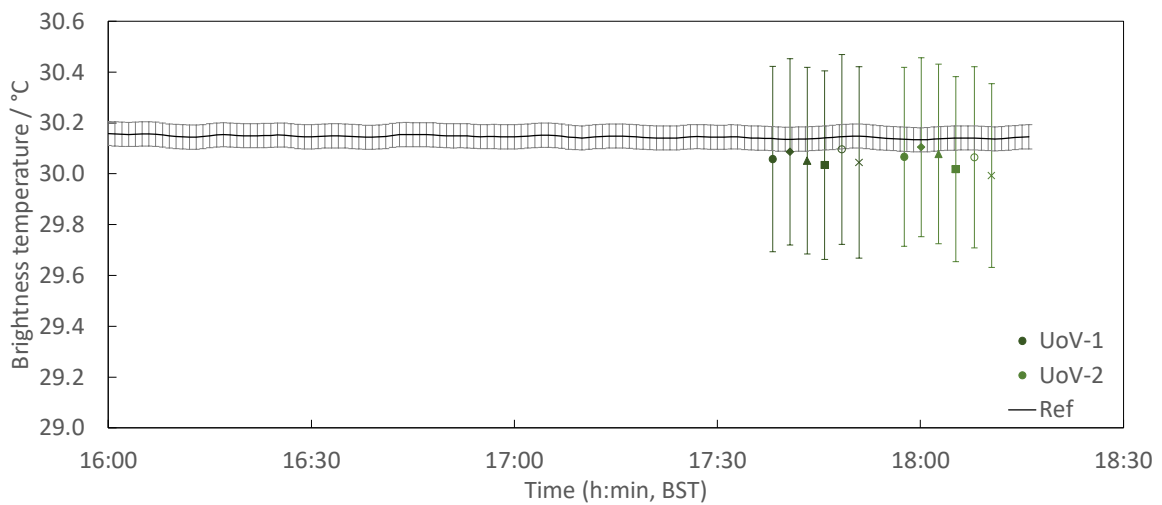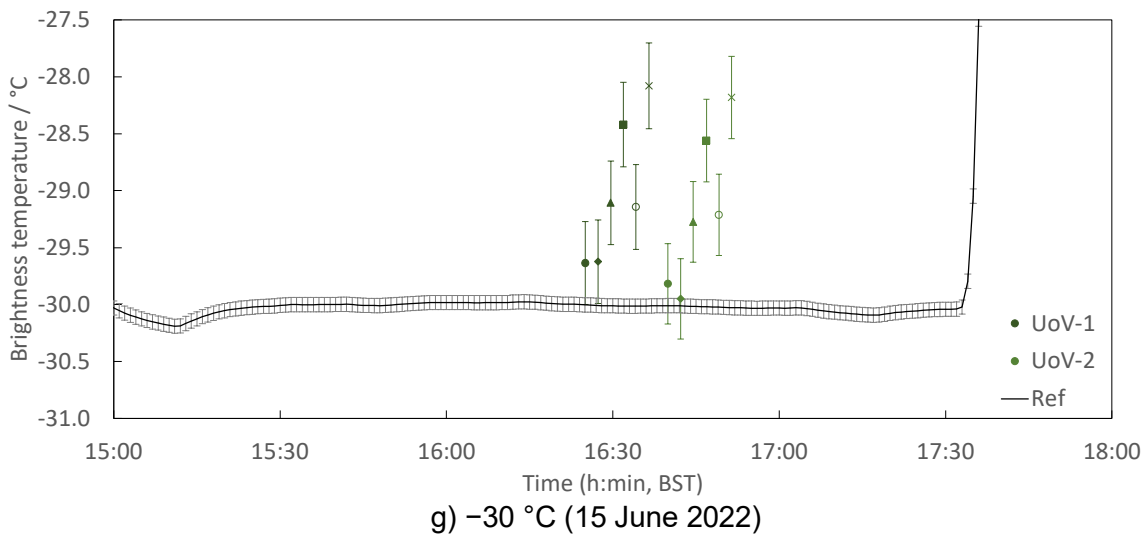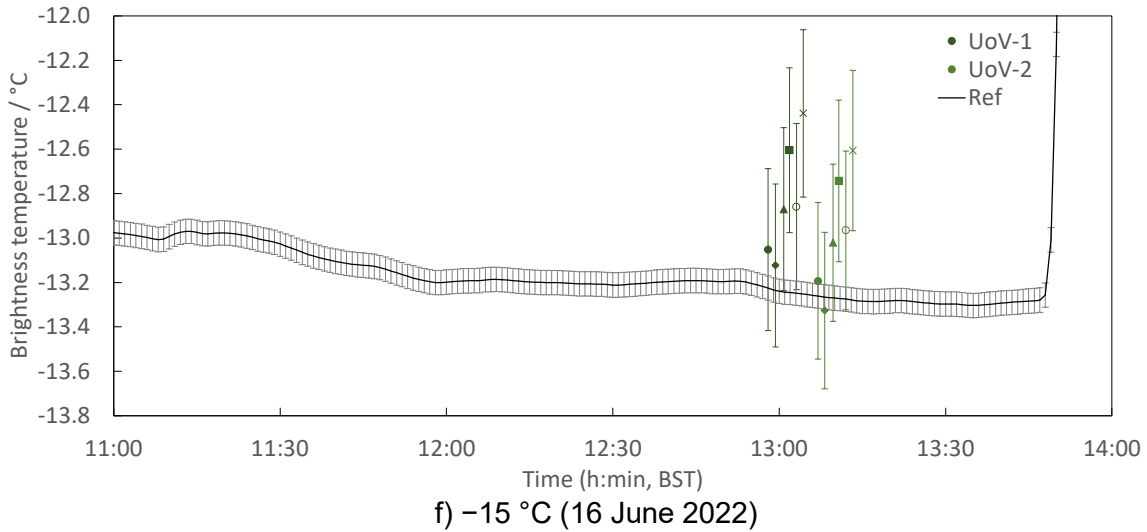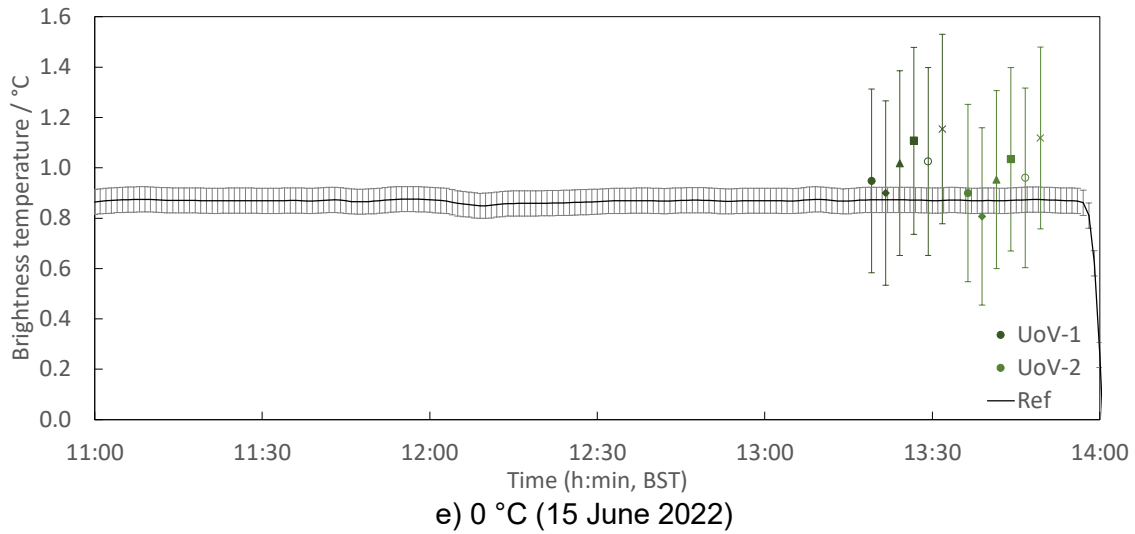to B6 in this order from left to right
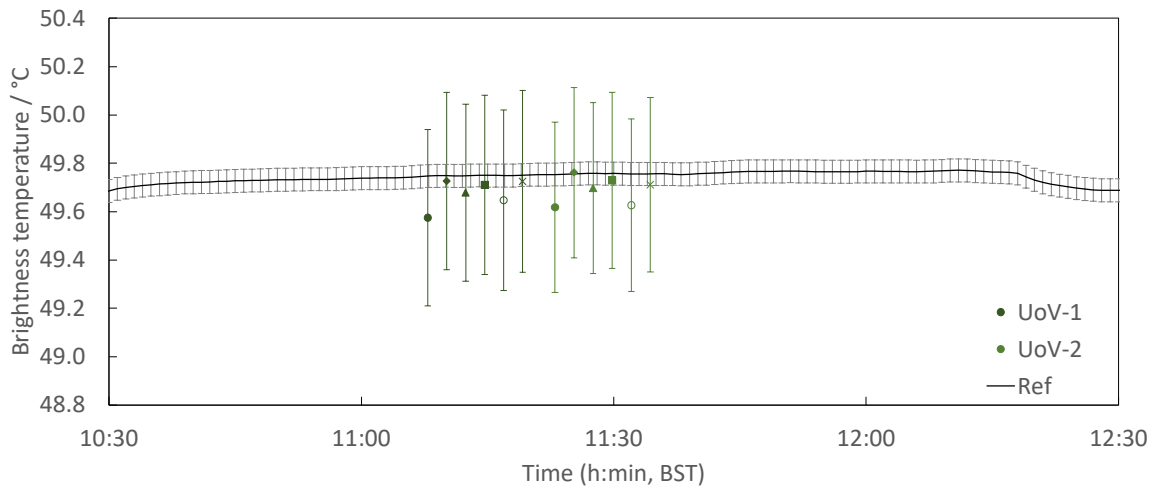
a) 50 °C (17 June 2022)
Figure 3 NH3-BB measurements by UoV (Error bar denotes standard uncertainty)
(Continued on next page)

10
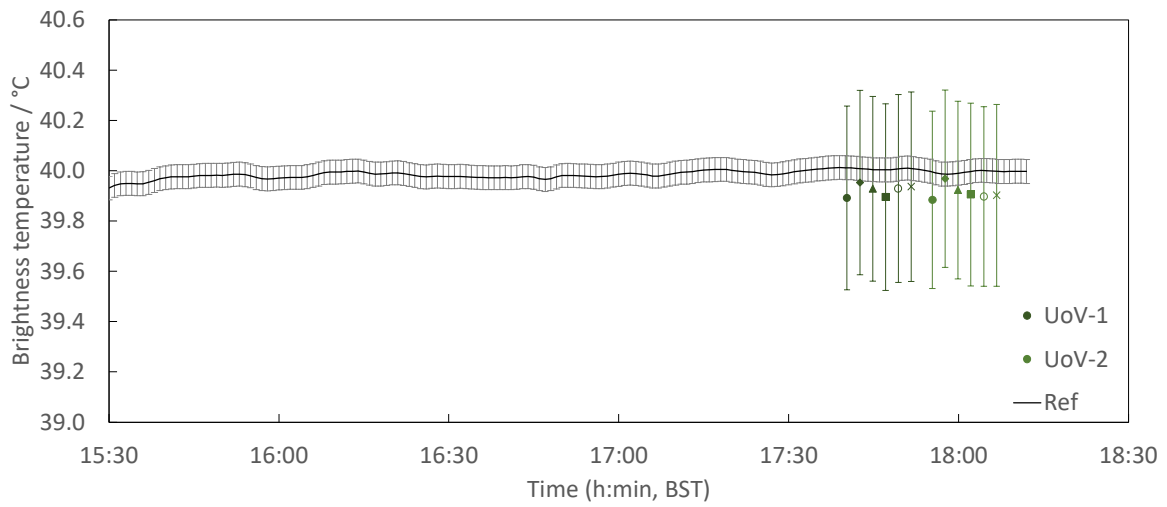
b) 40 °C (16 June 2022)

c) 35 °C (13 June 2022)

d) 30 °C (14 June 2022)

Figure 3 NH3-BB measurements by UoV (Error bar denotes standard uncertainty)
(Continued on next page)

e) 0 °C (15 June 2022)

f) −15 °C (16 June 2022)

g) −30 °C (15 June 2022)

Figure 3 NH3-BB measurements by UoV (Error bar denotes standard uncertainty) (cont.)
For both UoV-1 and UoV-2 radiometers, each plot corresponds to a spectral band, from B1
to B6 in this order from left to right.

5.2   MEASUREMENT BY KIT

5.2.1   Description of radiometers, route of traceability and uncertainty contributions

Make and type of Radiometers 'KIT-1' and 'KIT-2': Heitronics KT15.85 IIP

Outline Technical description of instrument: The KT15.85 IIP is a single channel radiometer based on a pyroelectric infrared detector. This type of sensor links radiance measurements via beam-chopping to internal reference temperature measurements and thermal drift can practically be eliminated. The KT15.85 IIP covers the spectral range from 9.6 µm to 11.5 µm, has an expanded uncertainty ($k = 2$) of about 0.3 K over the temperature range relevant to land surfaces and offers excellent long-term stability. The response time of the radiometer was set to 10 s. The type L6 lens used has a full-view angle of 8.3°. KIT-1 and KIT-2 only differ in their calibrated temperature ranges, which are from –25 °C to +100 °C and –100 °C to +100 °C, respectively.

Establishment or traceability route for primary calibration including date of last realisation and breakdown of uncertainty: Primary calibrations to within specifications were performed by Heitronics GmbH, Wiesbaden, Germany, on 2022-03-02 for KIT-1 (SN #9353; 'surface' radiometer) and on 2020-12-01 for KIT-2 (SN #13794; 'sky' radiometer) and verified using KIT's certified Landcal P80P blackbody. Breakdowns of uncertainties are provided in [AD-4].
The combined expanded uncertainty ($k = 2$) of the measurements made by the KIT radiometers during the current comparison was 380 mK to 400 mK in the temperature range of 10 °C to 30 °C.

Operational methodology during measurement campaign:
The radiometers were mounted on a tripod about 30 cm in front of the blackbody. For each measurement the radiometers were aligned with a laser target finder to view the centre of the blackbody's aperture.

Radiometer usage (deployment), previous use of instrument and planned applications.
The primary usage of the Heitronics KT15.85 IIP radiometers is the in-situ determination of land surface temperature (LST) at one of KIT's permanent satellite LST validation sites. Before deploying the radiometers to a site, the radiometers are re-calibrated against KIT's Landcal P80P blackbody. Radiometer #9353 (KIT-1) was previously deployed at Gobabeb, Namibia, and then overhauled and re-calibrated by the manufacturer; radiometer #13794 (KIT-2) has only been used in the laboratory. Both radiometers will replace currently deployed instruments.

Table 10 Uncertainty Contributions associated with Radiometers:
Instrument: Heitronics KT15.85 IIP
Temperature: 20 °C

| Uncertainty Contribution	Type A Uncertainty in Value / (appropriate units)	Type B Uncertainty in Value / (appropriate units)	Standard uncertainty in Brightness temperature / °C
Repeatability of measurement	0.12 %		0.024
	0.12 %		0.024

Reproducibility of measurement		0.150 °C	0.150
Primary calibration		0.053 °C	0.053
Linearity of radiometer		0.090 °C	0.090
Drift since calibration		0.035 °C	0.035
Ambient temperature fluctuations			
		0.035 °C	0.035
Atmospheric absorption/emission			
Combined uncertainty	0.17 %		0.192

Note: All uncertainty values are in standard uncertainties (i.e. *k* = 1)

Additional Type B uncertainty: 0.35 % of (target temp. – instrument temp.)

5.2.2 Measured data

Figures 4 and 5 show the measurement results reported by KIT for the SL-BB and for the NH3-BB, respectively. Two radiometer units are used. The two plots correspond to measurement with these units.
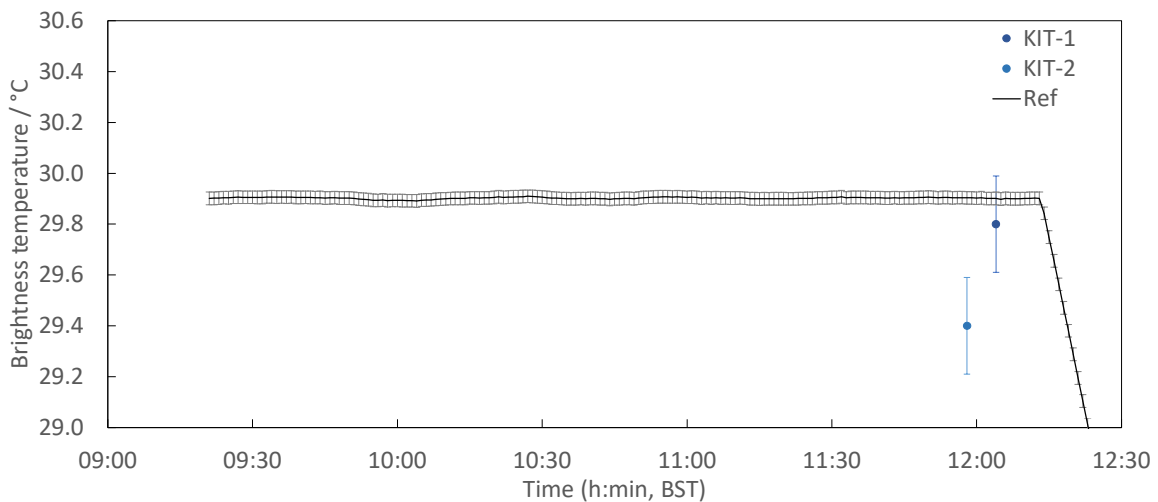
a) 30 °C (16 June 2022)

Figure 4 SL-BB measurements by KIT (Error bar denotes standard uncertainty) (continued on next page)
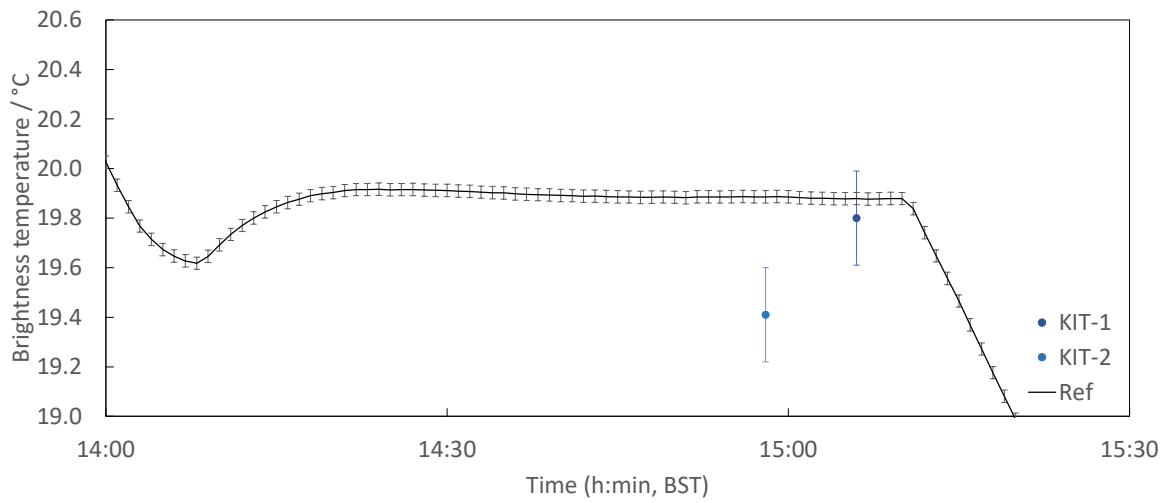
b) 20 °C (16 June 2022)
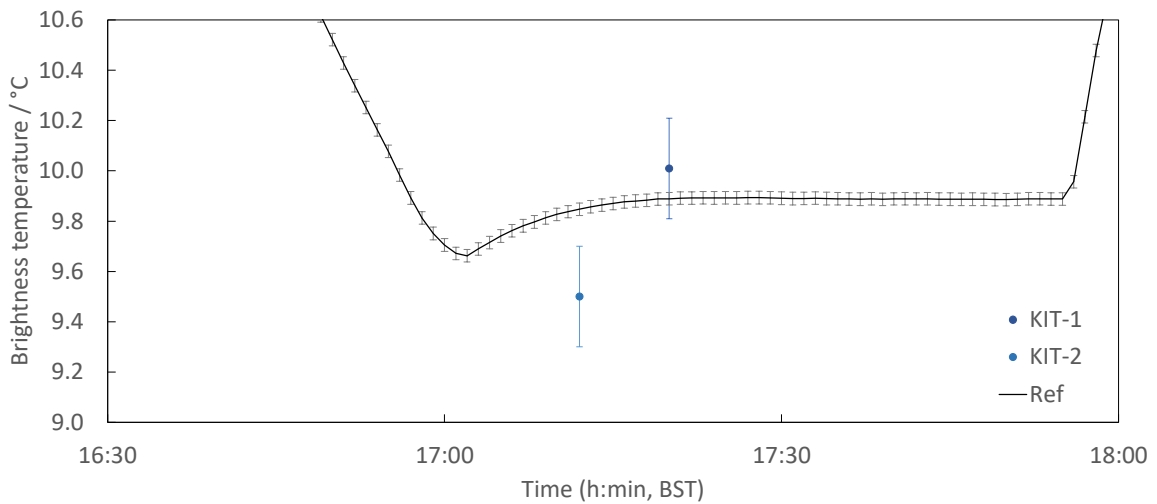
c) 10 °C (16 June 2022)
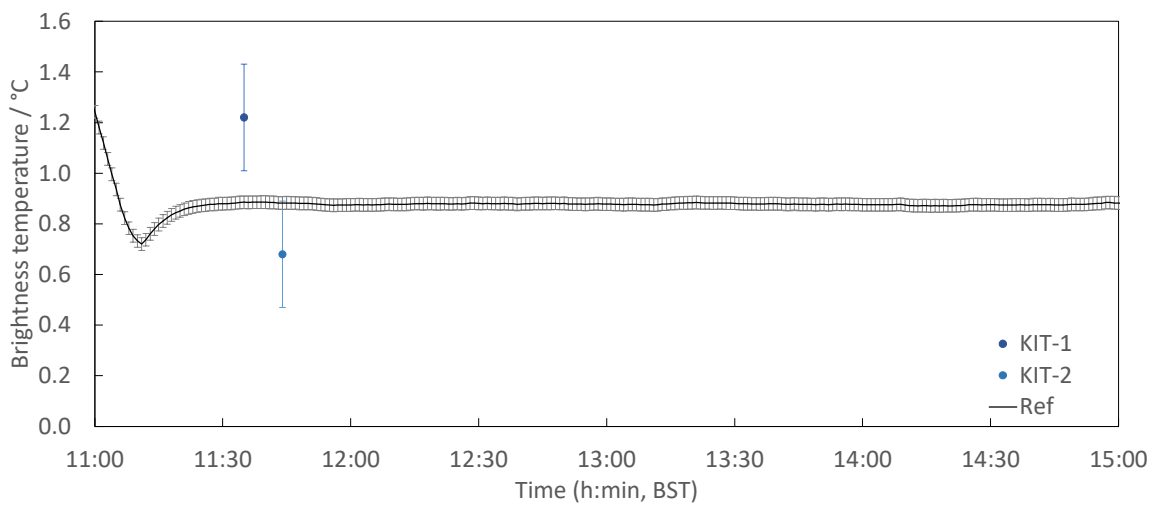
d) 0 °C (17 June 2022)

Figure 4 SL-BB measurements by KIT (Error bar denotes standard uncertainty) (cont.)
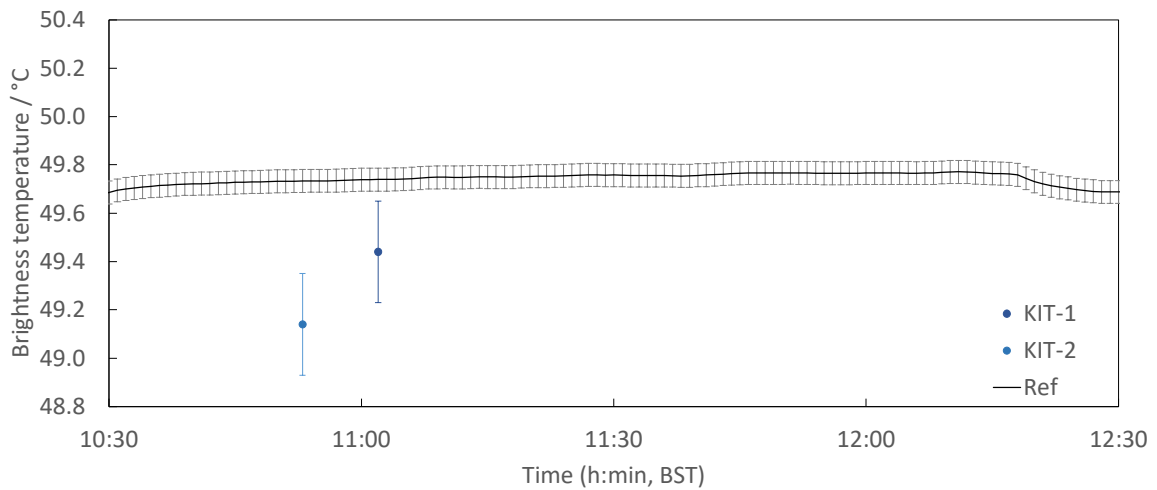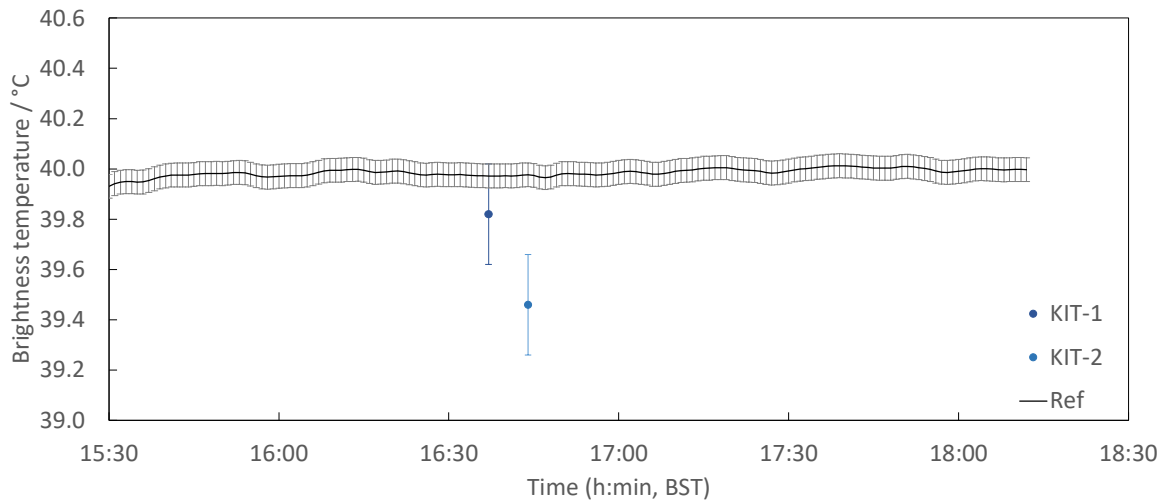
a) 50 °C (17 June 2022)
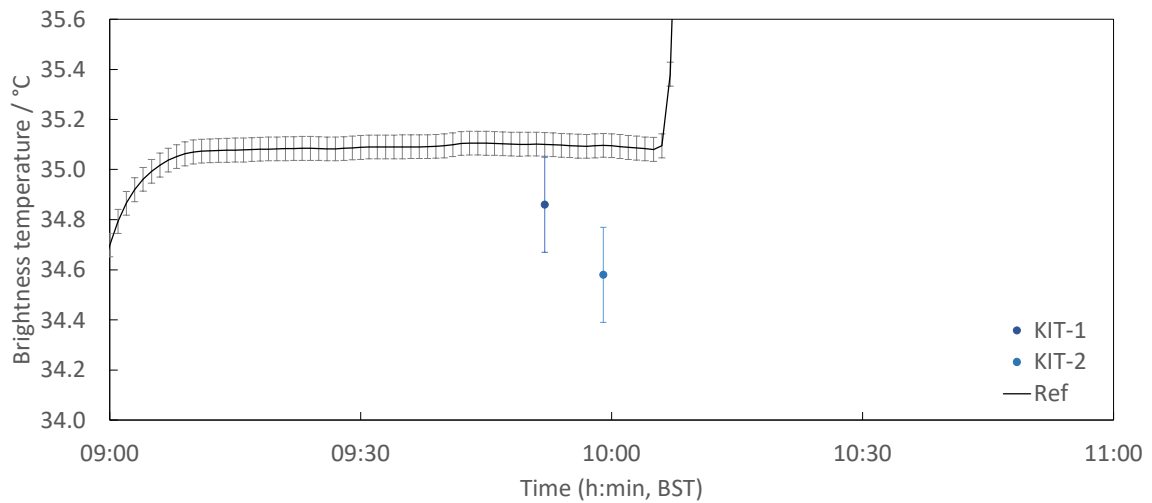
b) 40 °C (16 June 2022)

c) 35 °C (17 June 2022)

Figure 5 NH3-BB measurements by KIT (Error bar denotes standard uncertainty)
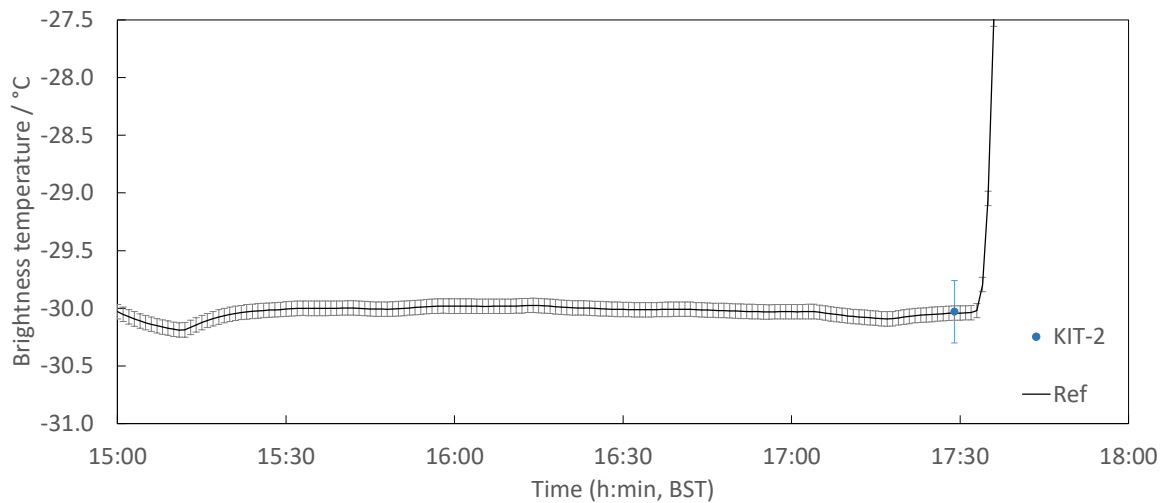(continued on next page)
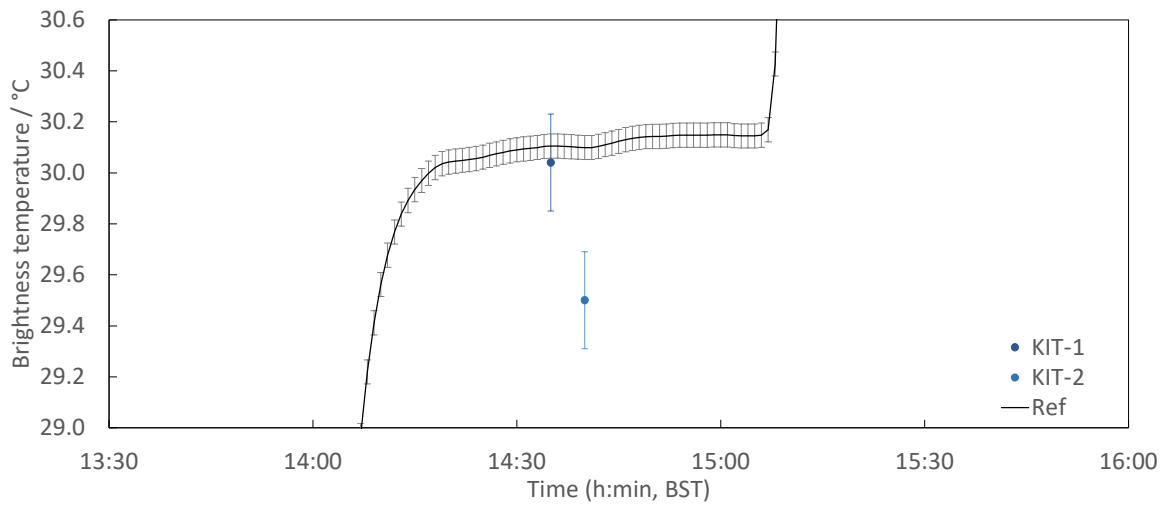
d) 30 °C (14 June 2022)
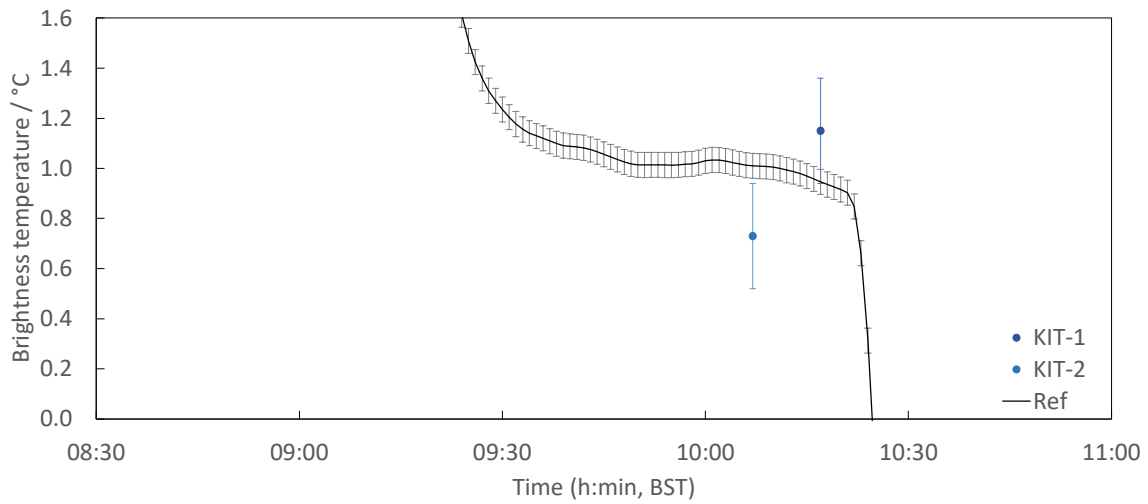
e) 0 °C (16 June 2022)
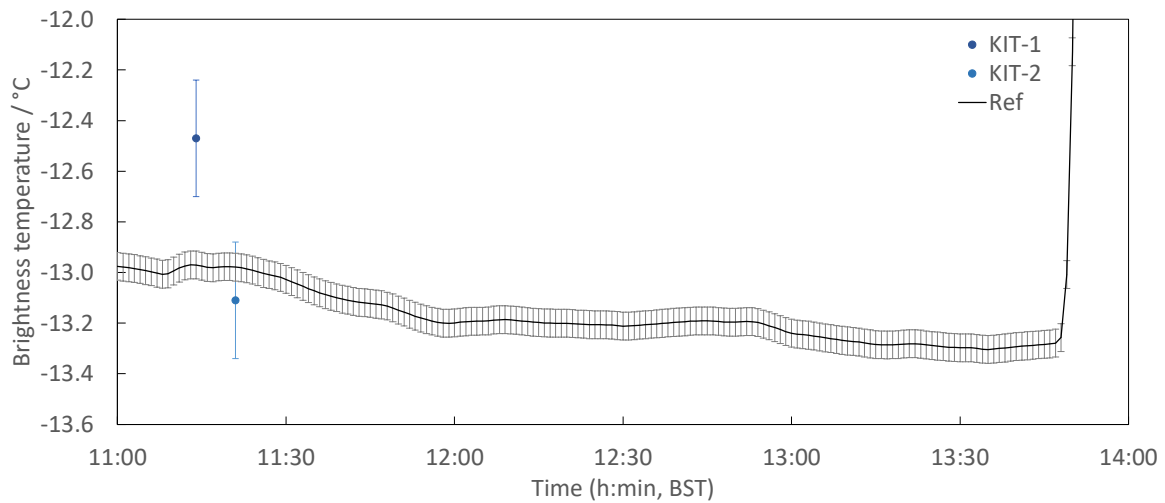
f) −15 °C (16 June 2022)

Figure 5 NH3-BB measurements by KIT (Error bar denotes standard uncertainty)
(continued on next page)

17

g) −30 °C (15 June 2022)
Figure 5 NH3-BB measurements by KIT (Error bar denotes standard uncertainty) (cont.)

5.3   MEASUREMENT BY CSIRO

5.3.1   Description of radiometer, route of traceability and uncertainty contributions

Make and type of Radiometer: ISAR5-E, serial number 16

Outline Technical description of instrument:
Type: ISAR Field of view: 3.5 degree half angle. Spectral band: 9.6 µm to 11.5 µm. Temperature resolution : 0.01 K.
Full information on the ISAR radiometer can be found in [15, 16].

Establishment or traceability route for primary calibration including date of last realisation and breakdown of uncertainty:
Last calibration: 19 June 2022 using CASOTS-II Blackbody (see [17])
Post calibration: 24 June 2022 using CASOTS-II Blackbody
The base line expanded uncertainty ($k = 2$) of ISAR is 50 mK as that is the uncertainty of BB thermistors and therefore the ISAR cannot have a lower uncertainty than that. The combined expanded uncertainty ($k = 2$) of the measurements made by the CSIRO ISAR radiometer during the comparison ranged from approximately 80 mK to 100 mK in the temperature range of 10 °C to 30 °C.
Full model on ISAR uncertainty is details in [16].

Operational methodology during measurement campaign:
The ISAR was installed on the custom trolley which is height adjustable to ensure the height is correct. The distance between the horizontal alignment dome nuts was measured to ensure the ISAR is installed on the same axis it was calibrated on.
The ISAR was running for at least half an hour in the measurement space to ensure there is no warm-up time required. The ISAR is autonomous and will operate in a regular 4 measurement cycle, two internal blackbodies, the sky view, and seaview, with 90 degrees from nadir being the seaview.
The ISAR was calibrated on 19 June 2022 after on-site repair and on the 24th June at the completion of this comparison and the data was processed using the data from both calibrations to adjust for any degradation in the optical components.

Radiometer usage (deployment), previous use of instrument and planned applications.
This ISAR will be installed on Research Vessel (RV) Investigator, an Australian Science Vessel.

Table 11 Uncertainty Contributions associated with Radiometer (CSIRO).

e	Item	Uncertainty	Unit	Type
1	Detector linearity	$<0.01\%$	K month^{-1}	B
2	Detector noise	~0.002	Volts	A
3	Detector accuracy	±0.5	K	B
4	ADC	$\pm1(\pm76.3)$	LSB (μV)	B
5	ADC accuracy	$\pm0.1\%$	Range	B
6	ADC zero drift	±6	μV $°C^{-1}$	B
7	Reference voltage 16-bit ADC	±15	mV	B
8	Reference voltage 12-bit ADC	±20	mV	B
9	Reference resistor	1	%	B
10	Reference resistor temperature coefficient	±100	Ppm $°C^{-1}$	B
11	BB emissivity	±0.000178	Emissivity	B
12	Sea surface emissivity	±0.07	Emissivity	B
13	Steinhart–Hart approximation	±0.01	K	B
14	Radiate transfer approximation	±0.001	K	B
15	Thermistor	±0.05	K	B
16	Thermistor noise	~0.002	V	A

Note: All uncertainty values are in standard uncertainties (i.e. $k = 1$)

5.3.2 Measured data

Figures 6 and 7 show the measurement results reported by CSIRO for the SL-BB and for the NH3-BB, respectively.
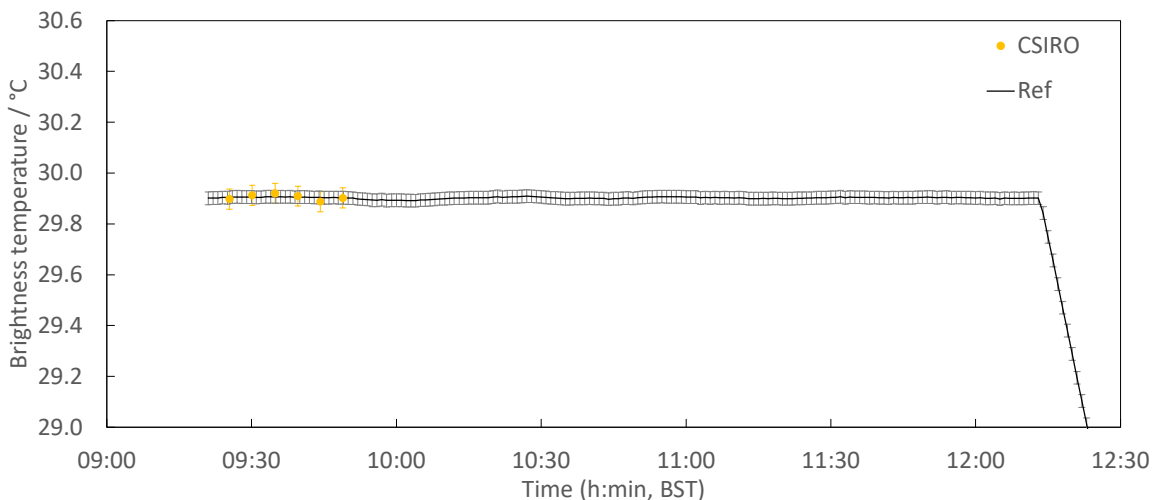
a) 30 °C (16 June 2022)
Figure 6 SL-BB measurements by CSIRO (Error bar denotes standard uncertainty)
(continued on next page)
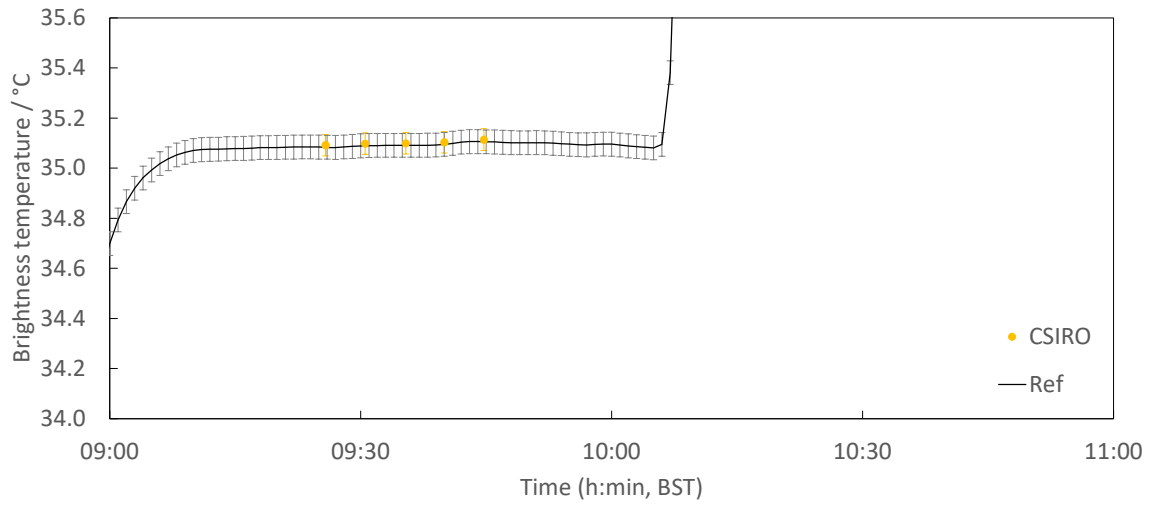
19
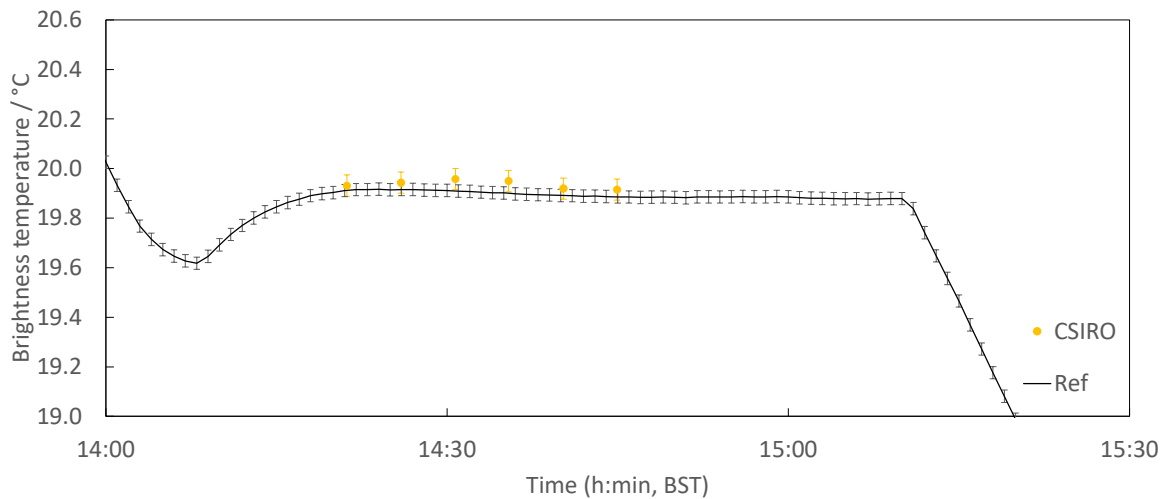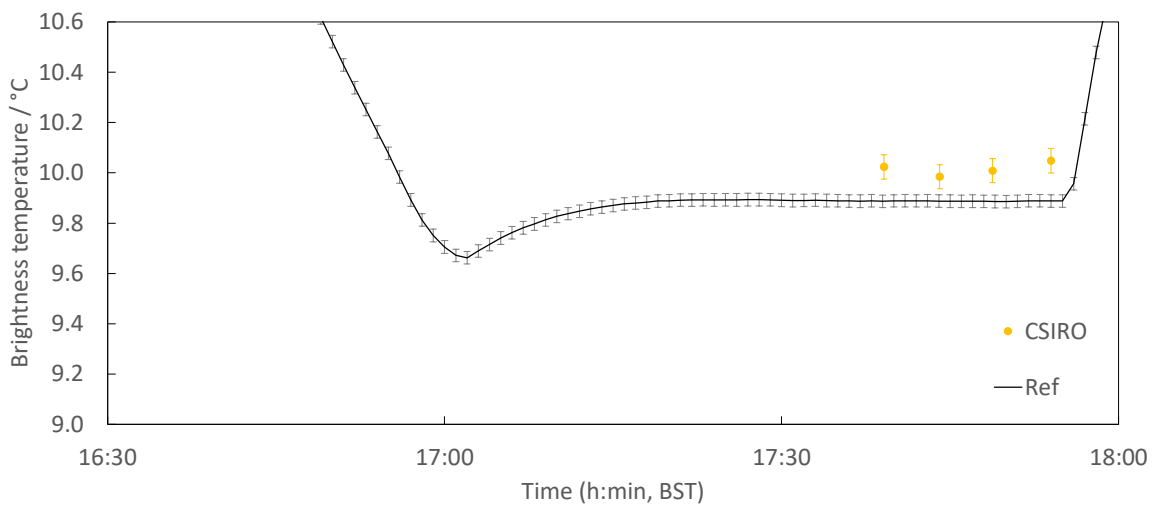
b) 20 °C (16 June 2022)
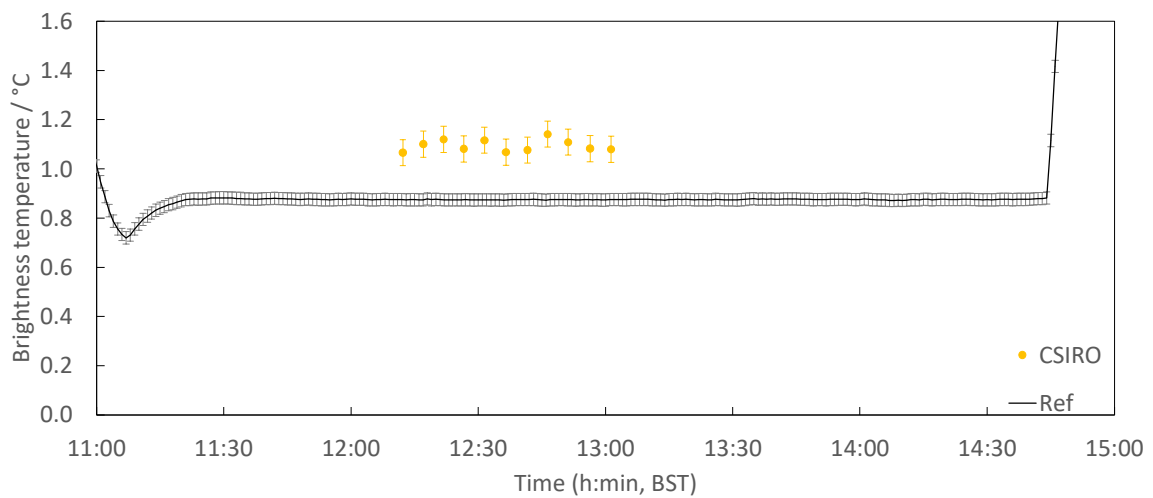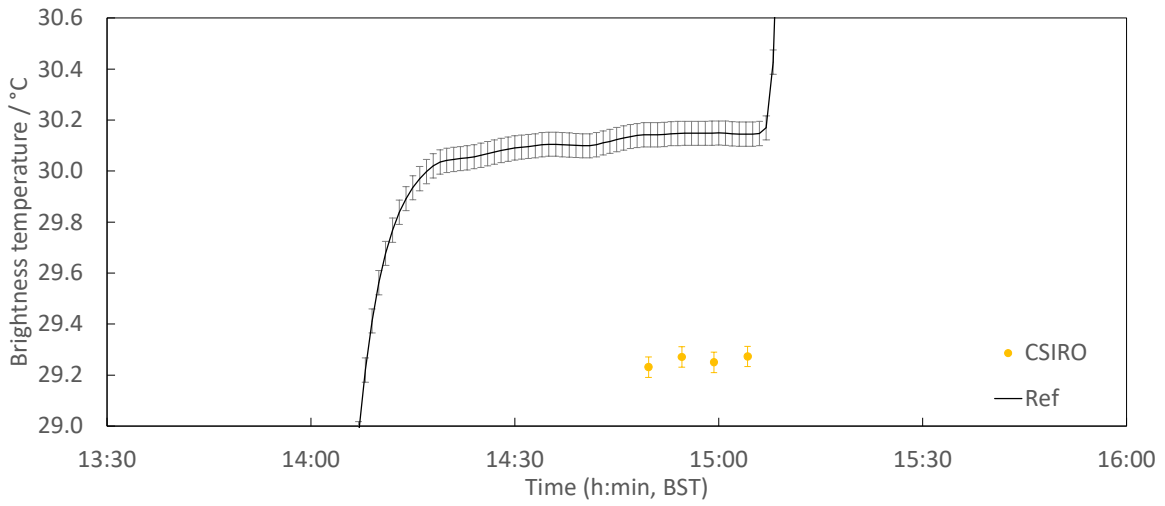

c) 10 °C (16 June 2022)
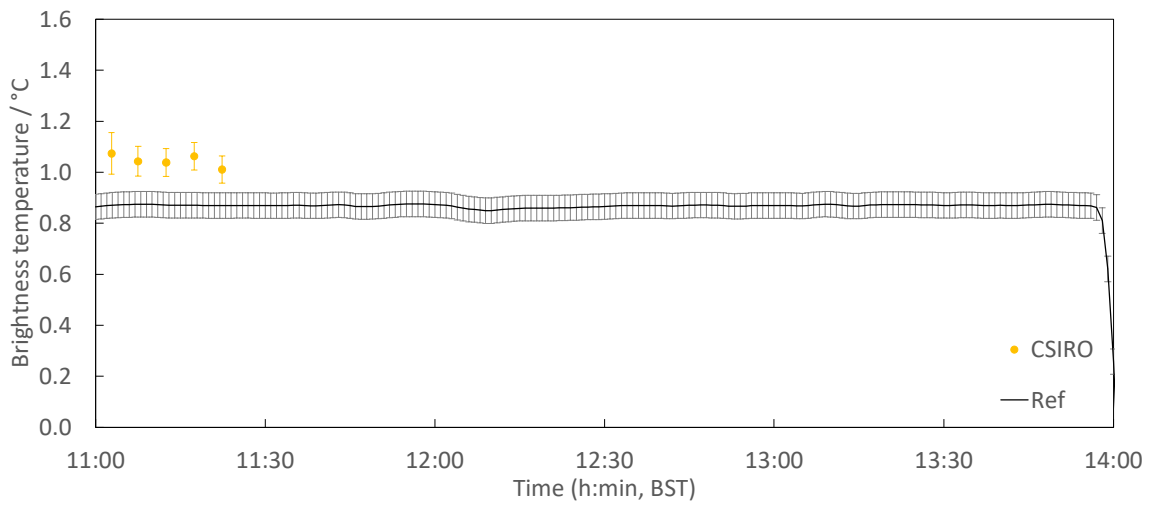

d) 0 °C (15 June 2022)

Figure 6 SL-BB measurements by CSIRO (Error bar denotes standard uncertainty)

a) 35 °C (17 June 2022)

b) 30 °C (16 June 2022)

c) 0 °C (15 June 2022)

Figure 7 NH3-BB measurements by CSIRO (Error bar denotes standard uncertainty)
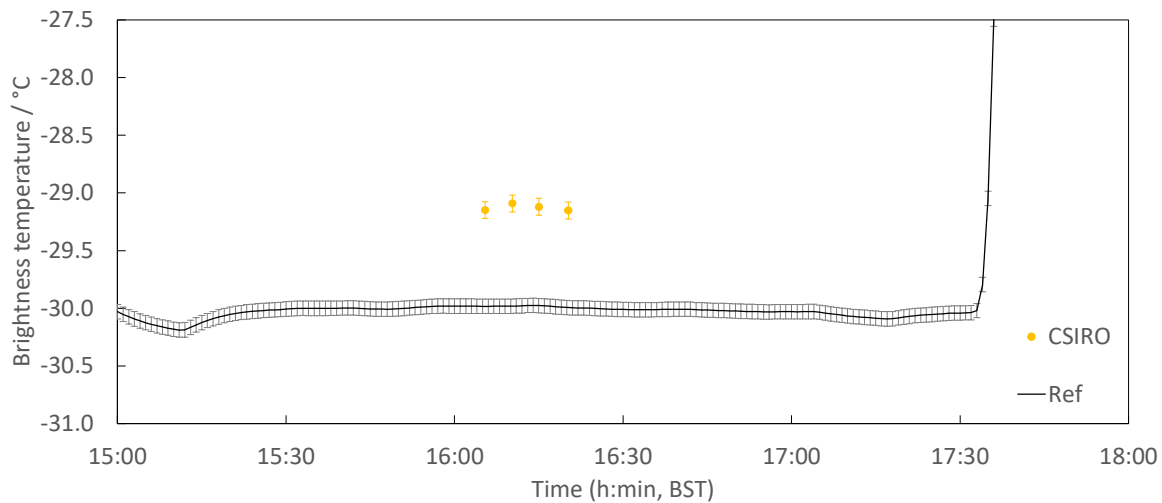(continued on next page)

d) −30 °C (15 June 2022)

Figure 7 NH3-BB measurements by CSIRO (Error bar denotes standard uncertainty) (cont.)

5.4   MEASUREMENT BY RAL

5.4.1   Description of radiometer, route of traceability and uncertainty contributions

The radiometer provided by the RAL was the Scanning Infrared Sea Surface Temperature Radiometer (SISTeR). SISTeR is a chopped, self-calibrating filter radiometer manufactured by RAL Space. It has a single-element DLaTGS pyroelectric detector, a filter wheel containing up to six band-defining filters and two internal reference BBs, one operating at ambient temperature and the other heated to approximately 17 K above ambient. During operation, the radiometer selected, with the aid of a scan mirror, successive views to each of the BBs and to the external scene in a repeated sequence. For SST measurements, the external measurements include views to the sea surface, and to the sky at the complementary angle. The instrument field of view is approximately 13° (full angle). During the comparison, a bandpass filter centred at 10.8 μm was used. The combined expanded uncertainty (k = 2) of the measurements made by the SISTeR radiometer during the comparison ranged from 25 mK to about 70 mK in the temperature range from 10 °C to 30 °C. Further information on the SISTeR radiometer can be found in [18].

5.4.2   Measured data

RAL has reported an issue with the performance of the SISTeR radiometer during check measurements after the comparison, which cannot be rectified in time for the publication of this report. Therefore, the results presented here should be considered preliminary and may require correction later.
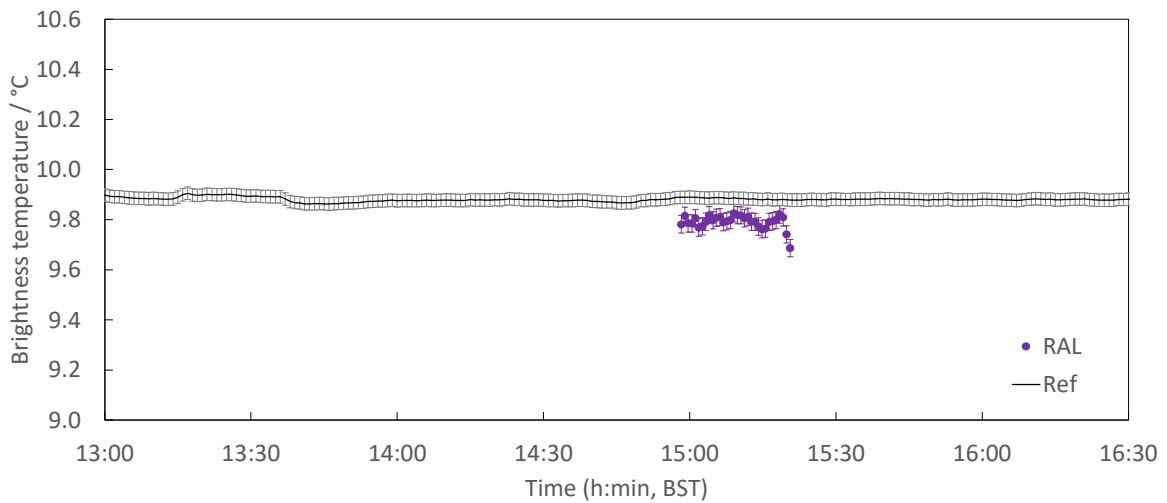
Figures 8 and 9 show the measurement results reported by RAL for the SL-BB and for the NH3-BB, respectively.
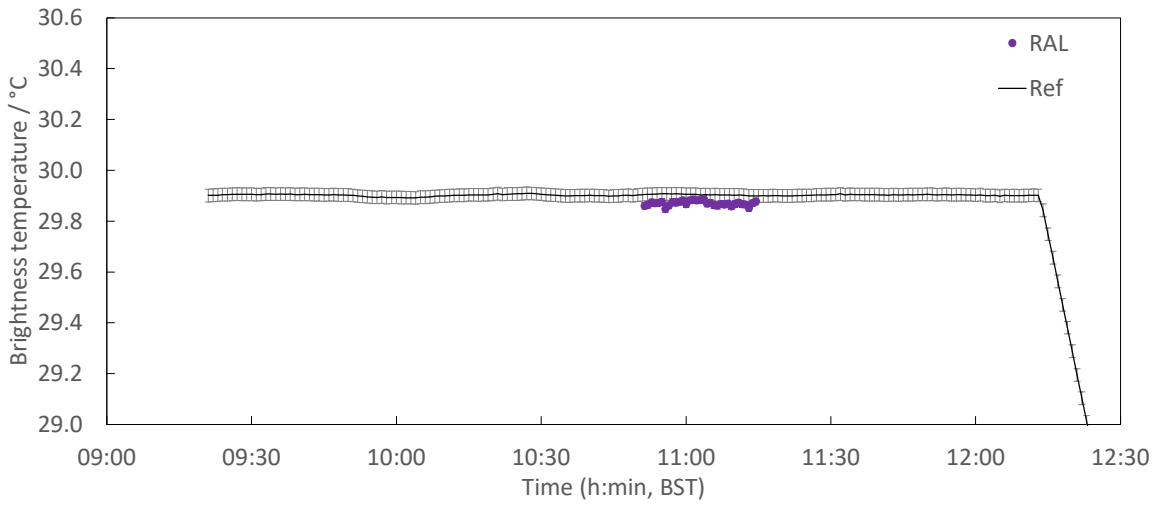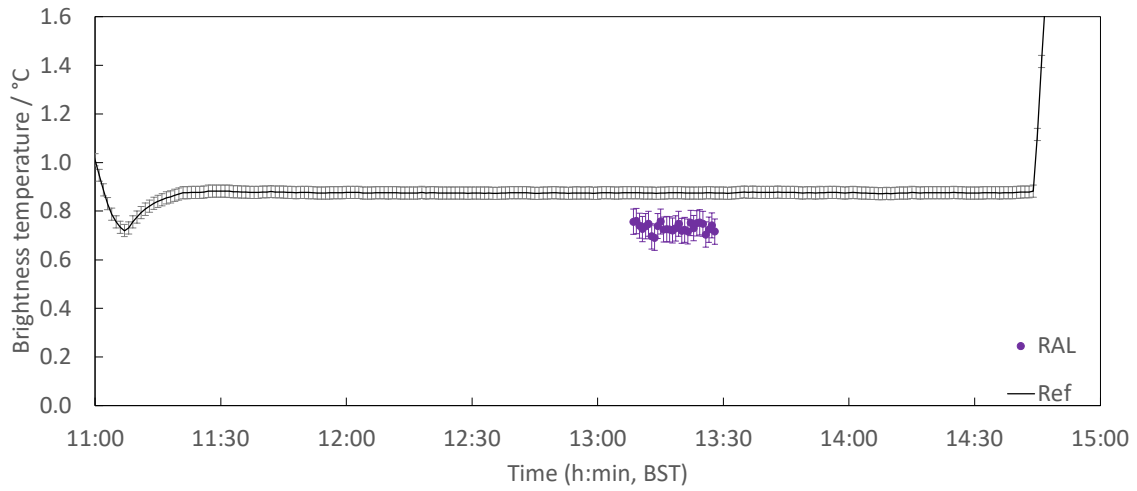
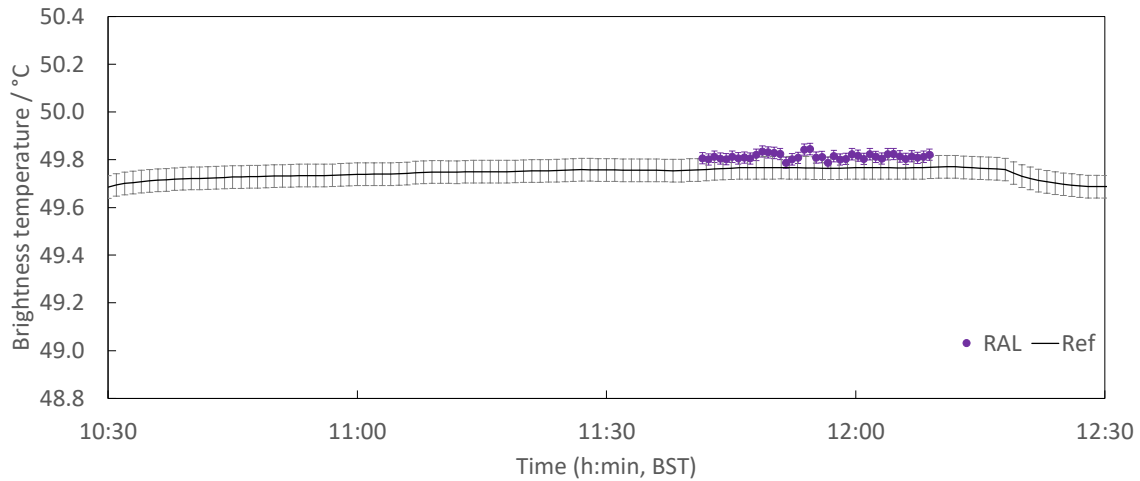a) 30 °C (16 June 2022)
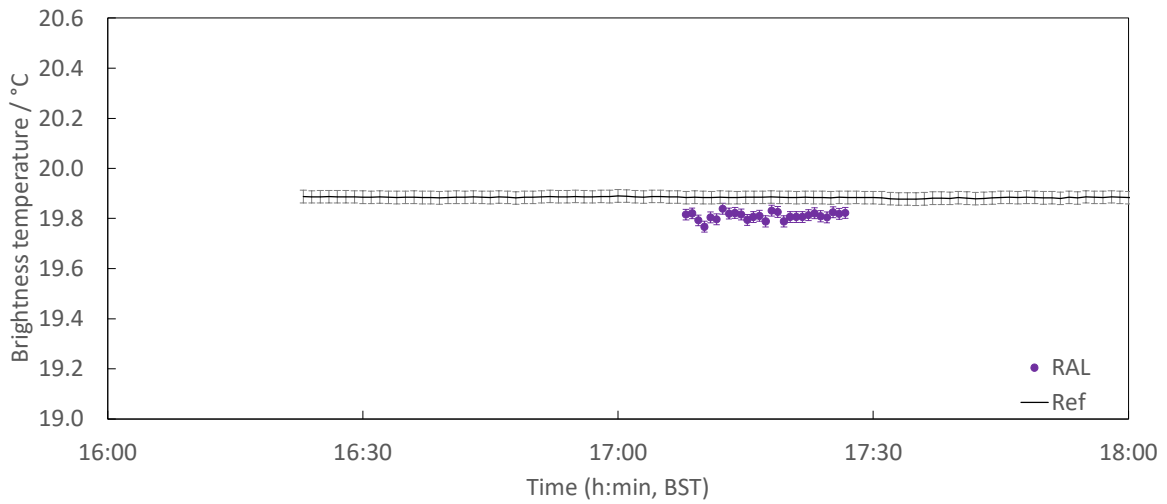
b) 20 °C (13 June 2022)

c) 10 °C (14 June 2022)

Figure 8 SL-BB measurements by RAL (Error bar denotes standard uncertainty) (continued on next page)
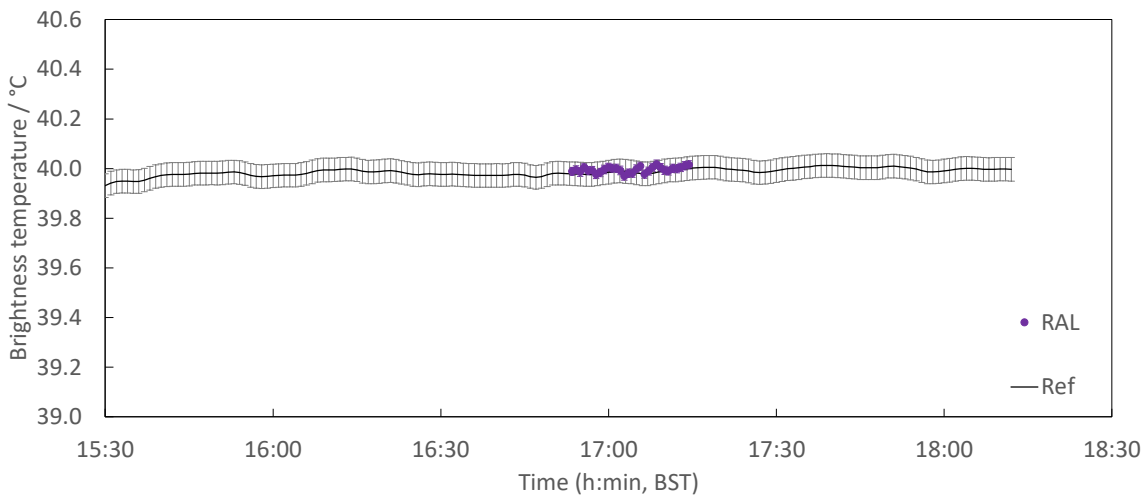
d) 0 °C (15 June 2022)

Figure 8 SL-BB measurements by RAL (Error bar denotes standard uncertainty) (cont.)
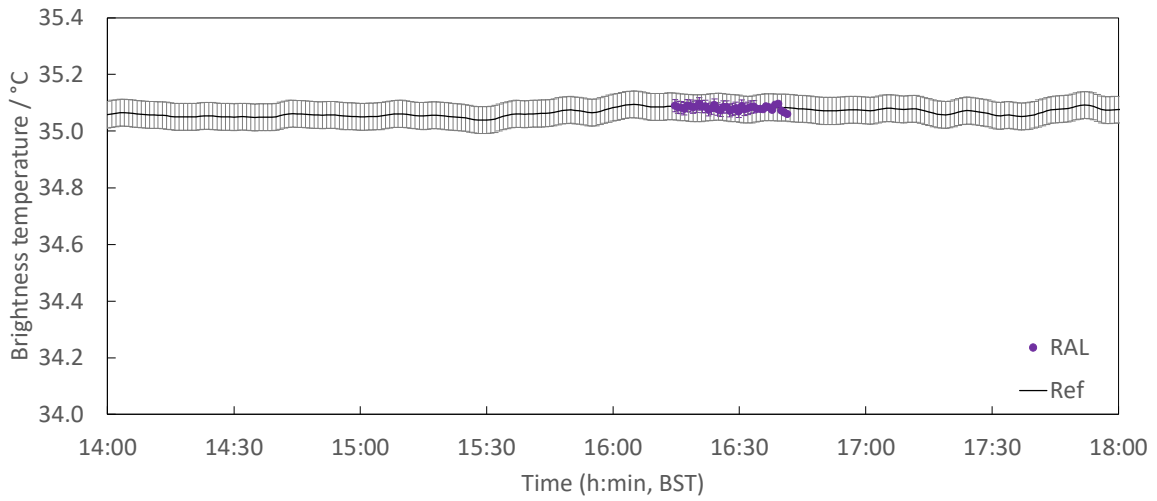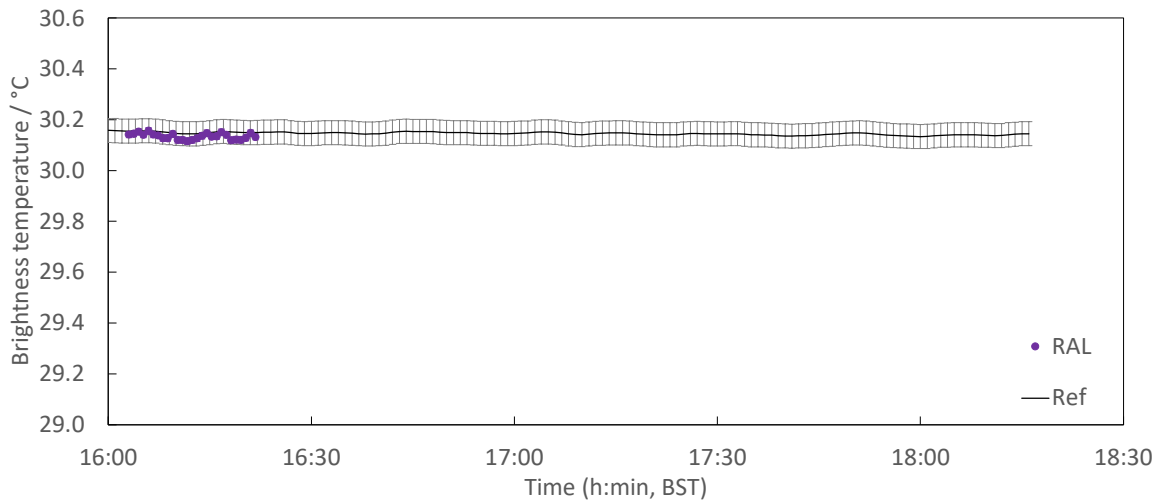

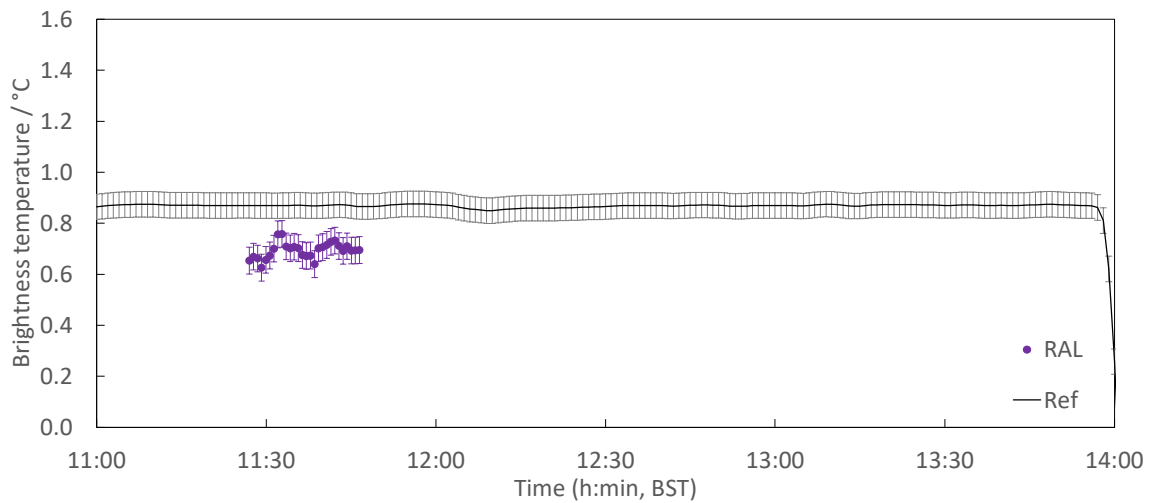
a) 50 °C (17 June 2022)

b) 40 °C (16 June 2022)

Figure 9 NH3-BB measurements by RAL (Error bar denotes standard uncertainty)
(continued on next page)

24

c) 35 °C (13 June 2022)

d) 30 °C (14 June 2022)

e) 0 °C (15 June 2022)

Figure 9 NH3-BB measurements by RAL (Error bar denotes standard uncertainty)
(continued on next page)

f) −15 °C (16 June 2022)
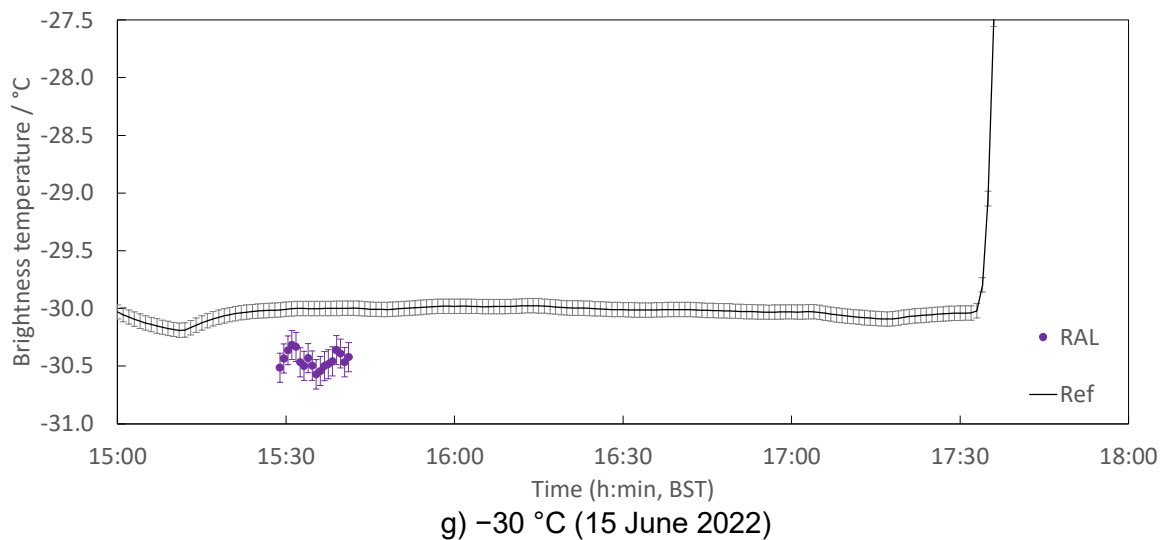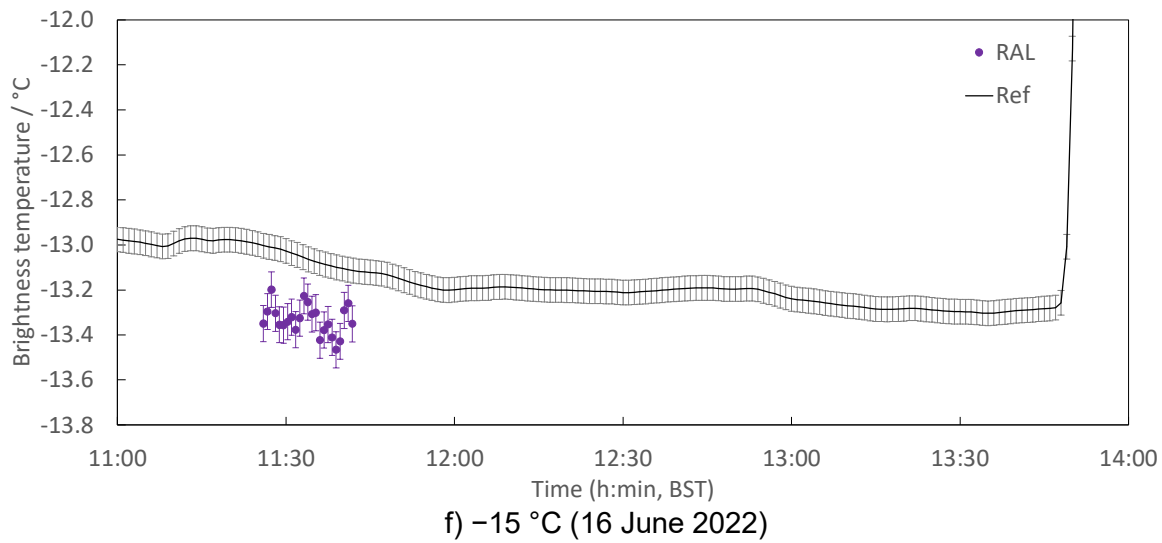

g) −30 °C (15 June 2022)

Figure 9 NH3-BB measurements by RAL (Error bar denotes standard uncertainty) (cont.)

5.5   MEASUREMENT BY UoS

5.5.1   Description of radiometer, route of traceability and uncertainty contributions

Make and type of Radiometer: ISAR5-C serial number 3

Outline Technical description of instrument:
The ISAR (Infrared Sea surface temperature Autonomous Radiometer) is a self-calibration scanning radiometer, measuring at a single waveband between 9.6 µm to 11.5 µm. It uses two BBs for the calibration of the detector, one at ambient temperature and one at approximately 12 K above ambient temperature. The detector is a Heitronics KT15 with a field of view of 7 degrees. A detailed description of the ISAR radiometer can be found in [15,16].

Establishment or traceability route for primary calibration including date of last realisation and breakdown of uncertainty:

26

The traceability route for ISAR is through the internal BB thermistors which are traceable to NIST. The internal calibration is verified with an external water BB (CASOTS-II, see [17]) before and after each deployment. Both ISAR and CASOTS get verified by NPL every five to six years at the radiometer inter-comparisons to ensure their performance and uncertainty.

The ISAR uncertainty model is described in [16] and propagates the uncertainties of each component through the measurement equation. This produces a per measurement uncertainty, which is split into Type A and Type B uncertainties as well as an instrument and a measurement uncertainty. Figure 10 shows a flow chart of the uncertainty components propagated through the measurement equation and Table 12 shows the associated uncertainties of the main components. The base line expanded uncertainty ($k = 2$) of ISAR is 50 mK as that is the uncertainty of BB thermistors and therefore the ISAR cannot have a lower uncertainty than that. The combined expanded uncertainty ($k = 2$) of the measurements made by the UoS ISAR radiometer during the comparison ranged from approximately 80 mK to 110 mK in the temperature range from 10 °C to 30 °C.
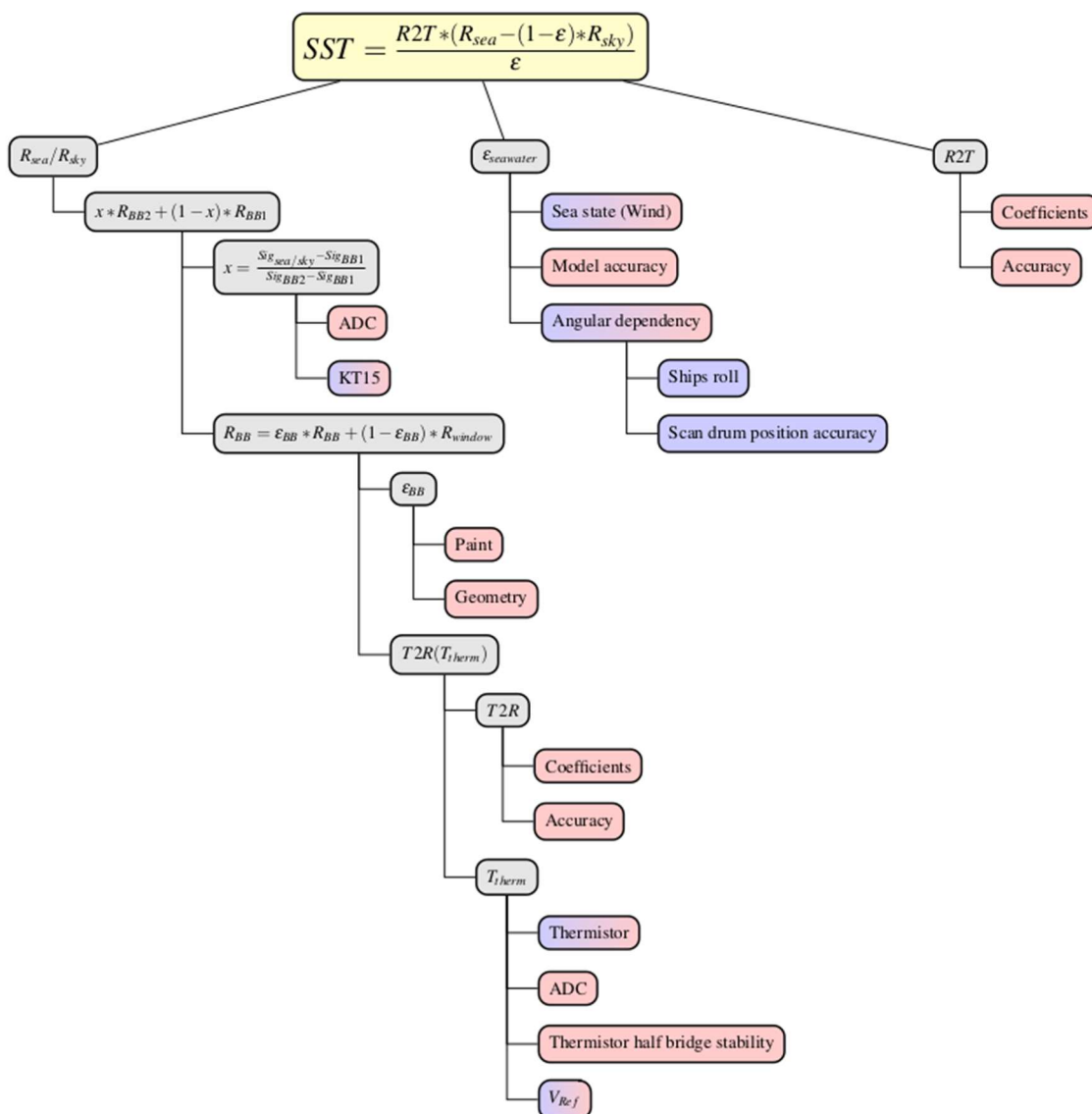

Figure 10 ISAR uncertainty model, from [16]

Table 12 Uncertainty Contributions associated with Radiometer (UoS).

e	Item	Uncertainty	Unit	Type
1	Detector linearity	<0.01%	K month^{-1}	B
2	Detector noise	~0.002	Volts	A
3	Detector accuracy	±0.5	K	B
4	ADC	±1(±76.3)	LSB (μV)	B
5	ADC accuracy	±0.1%	Range	B
6	ADC zero drift	±6	μV°C^{-1}	B
7	Reference voltage 16-bit ADC	±15	mV	B
8	Reference voltage 12-bit ADC	±20	mV	B
9	Reference resistor	1	%	B
10	Reference resistor temperature coefficient	±100	Ppm°C^{-1}	B
11	BB emissivity	±0.000178	Emissivity	B
12	Sea surface emissivity	±0.07	Emissivity	B
13	Steinhart–Hart approximation	±0.01	K	B
14	Radiate transfer approximation	±0.001	K	B
15	Thermistor	±0.05	K	B
16	Thermistor noise	~0.002	V	A

Note: All uncertainty values are in standard uncertainties (i.e. k = 1)

Operational methodology during measurement campaign:
The ISAR was installed on a custom trolley which is height adjustable to ensure the height is correct. The distance between the horizontal alignment dome nuts was measured to ensure the ISAR is installed on the same axis it was calibrated on.
The ISAR was running for at least half an hour in the measurement space to ensure there is no warmup time required. The ISAR is autonomous and operates in a regular 4 measurement cycle, two internal blackbodies, the sky view, and seaview, with 90 degrees from nadir being the seaview.
The data was processed after a post workshop calibration had been completed, to adjust for any changes in the optical components.
The ISAR was calibrated against the UoS CASOTS-II before the NPL measurements and again after the Boscombe pier deployment to ensure it was operating correctly during the measurements.
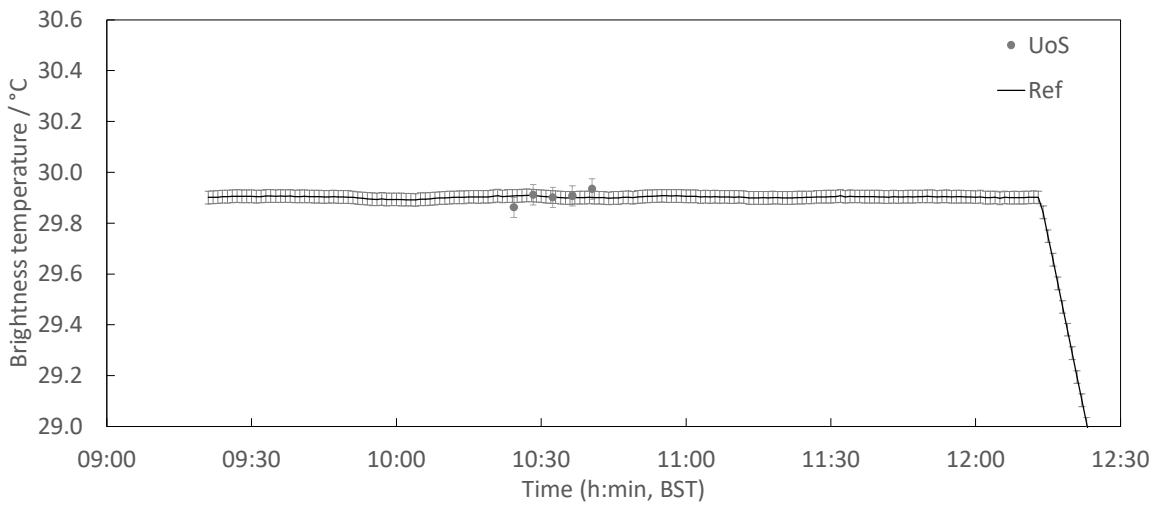
Radiometer usage (deployment), previous use of instrument and planned applications.
The UoS ISARs (S/N 2,3 and 12) are mainly used on ferries traveling between the UK and Spain, but are also used on mainly UK research vessels and on opportunistic measurement campaigns on ICE (Greenland 2011 and 2016 or land Namibia 2017).
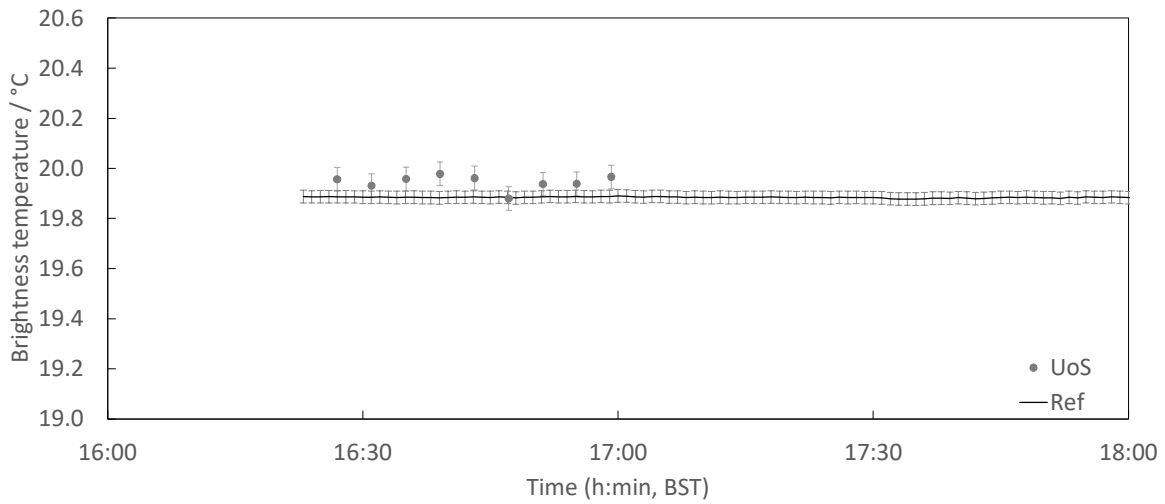
The UoS ISAR data is processed to the International SST FRM Radiometer Network (ISFRN) Level 2 in situ radiometric data product (L2R) netcdf data format and stored at the ships4sst archive at National Institute for Ocean Science (IFREMER). These data are used by European Organisation for the Exploitation of Meteorological Satellites (EUMETSAT) to produce the validation match-up database for the Sea and Land Surface Temperature Radiometer (SLSTR) sensor on the ESA Sentinel 3 satellite.
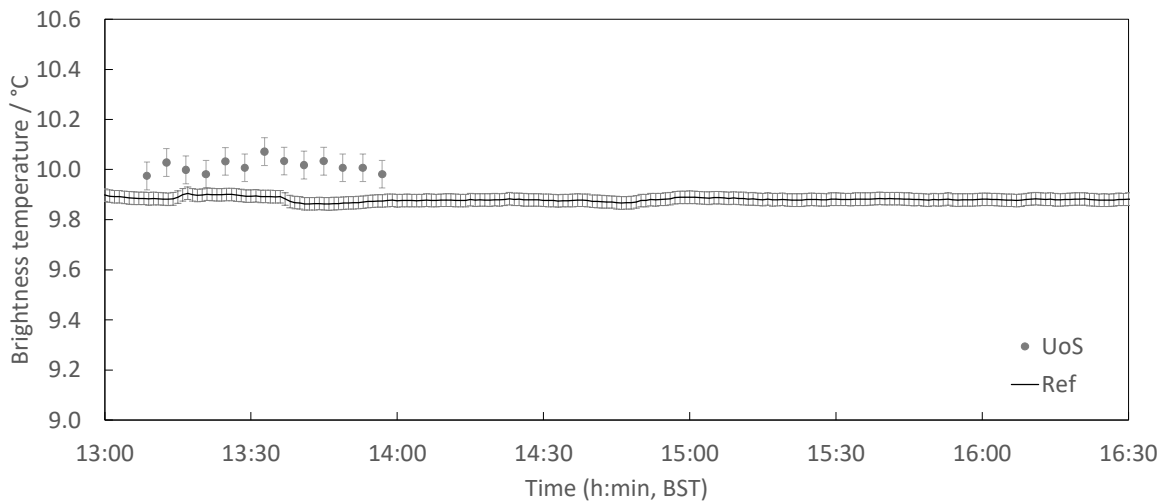

5.5.2   Measured data

Figures 11 and 12 show the measurement results reported by UoS for the SL-BB and for the NH3-BB, respectively.

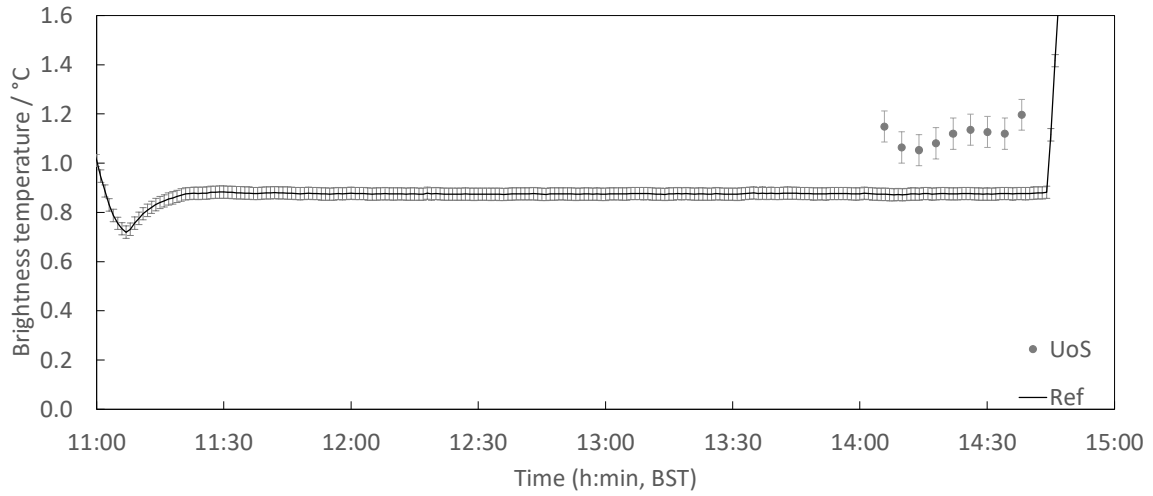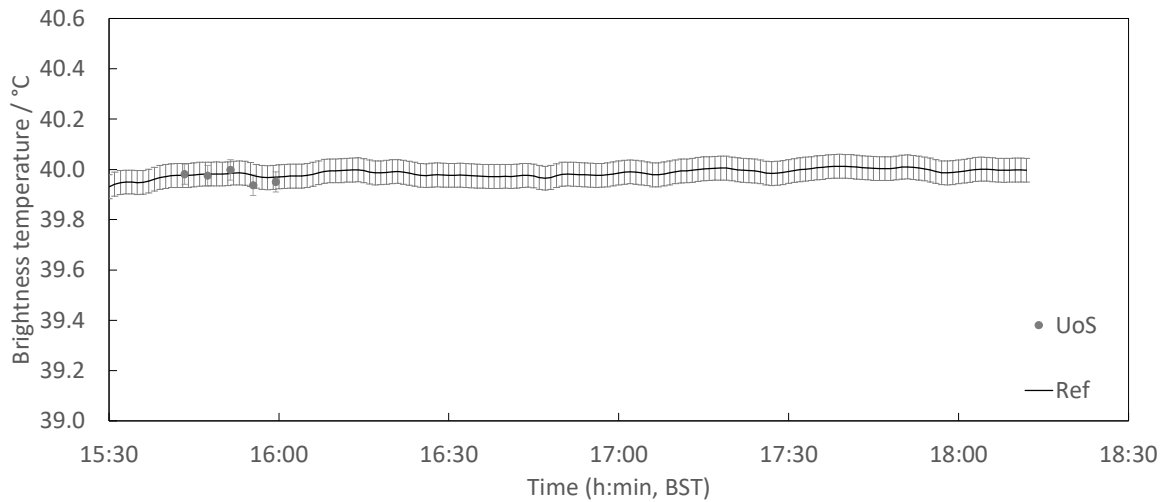a) 30 °C (16 June 2022)

b) 20 °C (13 June 2022)

c) 10 °C (14 June 2022)

Figure 11 SL-BB measurements by UoS (Error bar denotes standard uncertainty)
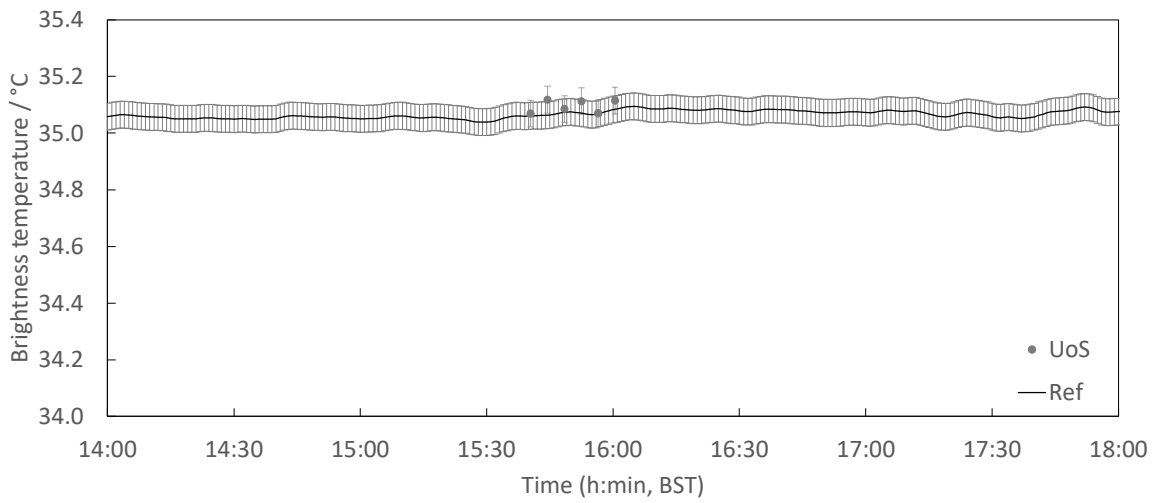(continued on next page)

d) 0 °C (15 June 2022)

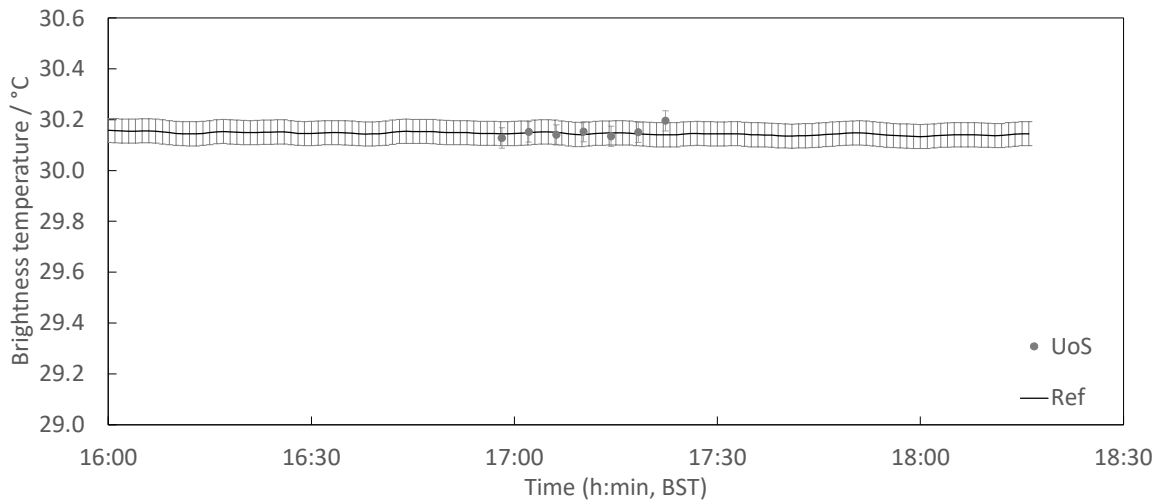Figure 11 SL-BB measurements by UoS (Error bar denotes standard uncertainty) (cont.)
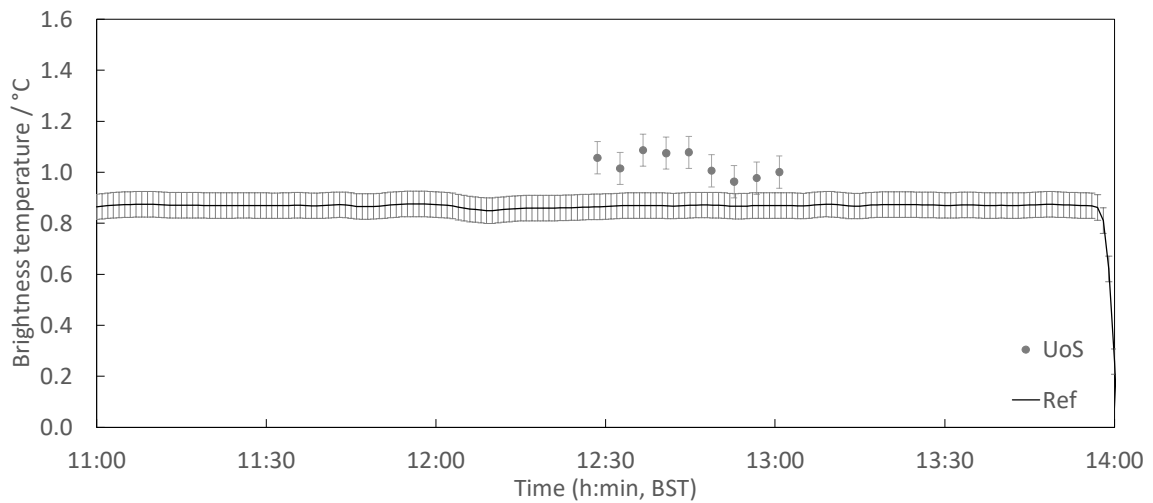

a) 40 °C (16 June 2022)

Figure 12 NH3-BB measurements by UoS (Error bar denotes standard uncertainty)
(continued on next page)

b) 35 °C (13 June 2022)

c) 30 °C (14 June 2022)

d) 0 °C (15 June 2022)

Figure 12 NH3-BB measurements by UoS (Error bar denotes standard uncertainty)
(continued on next page)

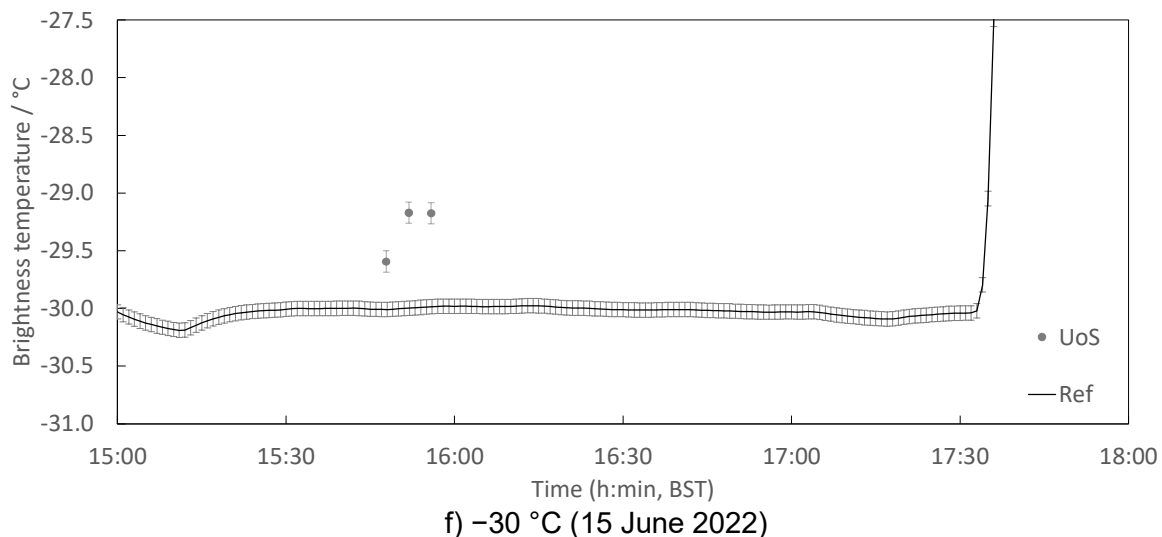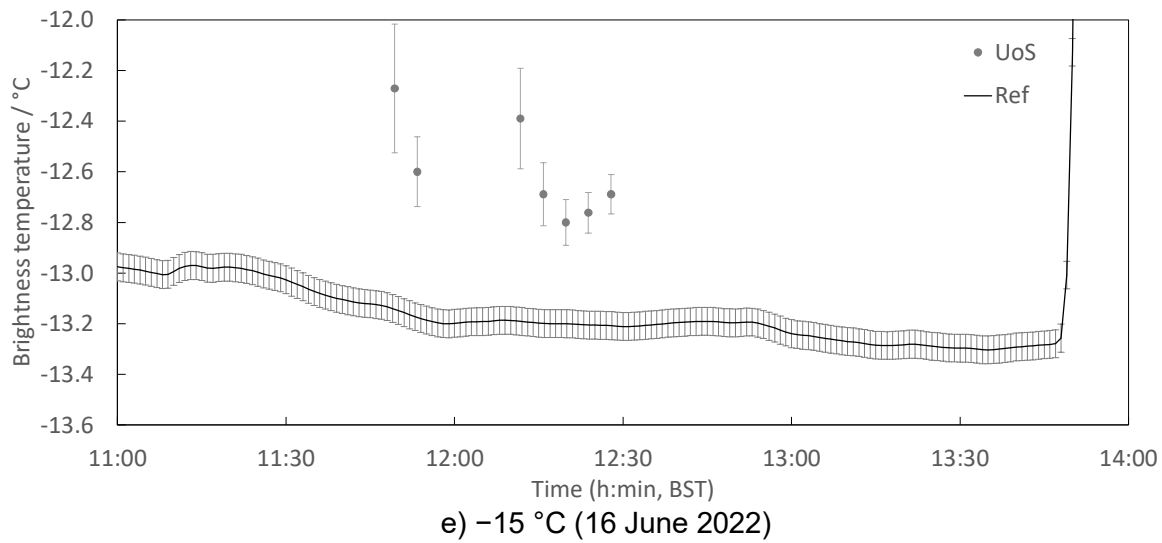e) −15 °C (16 June 2022)

f) −30 °C (15 June 2022)

Figure 12 NH3-BB measurements by UoS (Error bar denotes standard uncertainty) (cont.)
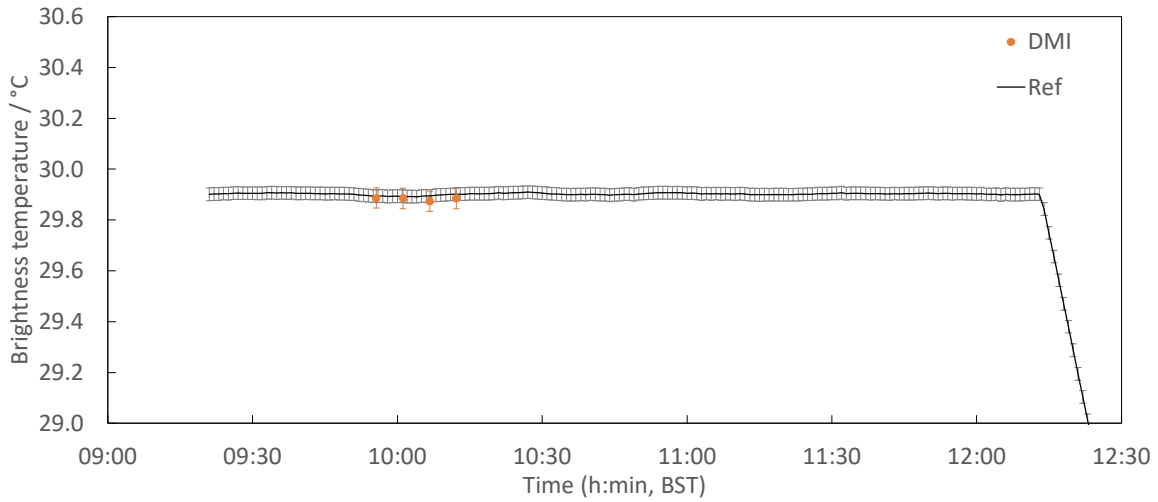
5.6   MEASUREMENT BY DMI

5.6.1   Description of radiometer, route of traceability and uncertainty contributions

The radiometer provided by the DMI for the current comparison was an ISAR-5D. This is a self-calibration scanning radiometer, measuring at a single waveband between 9.6 μm to 11.5 μm. It uses two BBs for the calibration of the detector, one at ambient temperature and one at approximately 12 K above ambient temperature. The detector is a Heitronics KT15 with a field of view of 7 degrees. A detailed description of the ISAR radiometer can be found in [15,16].

This radiometer was calibrated with the aid of a CASOTS-II blackbody [17]. A full breakdown of the combined uncertainty associated with the measurement of the SST using ISAR can be found in [16]. The combined expanded uncertainty ($k = 2$) of the measurements made by the DMI ISAR during the current comparison was approximately 80 mK to 100 mK in the temperature range of 10 °C to 30 °C.

5.6.2 Measured data

Figures 13 and 14 show the measurement results reported by DMI for the SL-BB and for the NH3-BB, respectively.

a) 30 °C (16 June 2022)
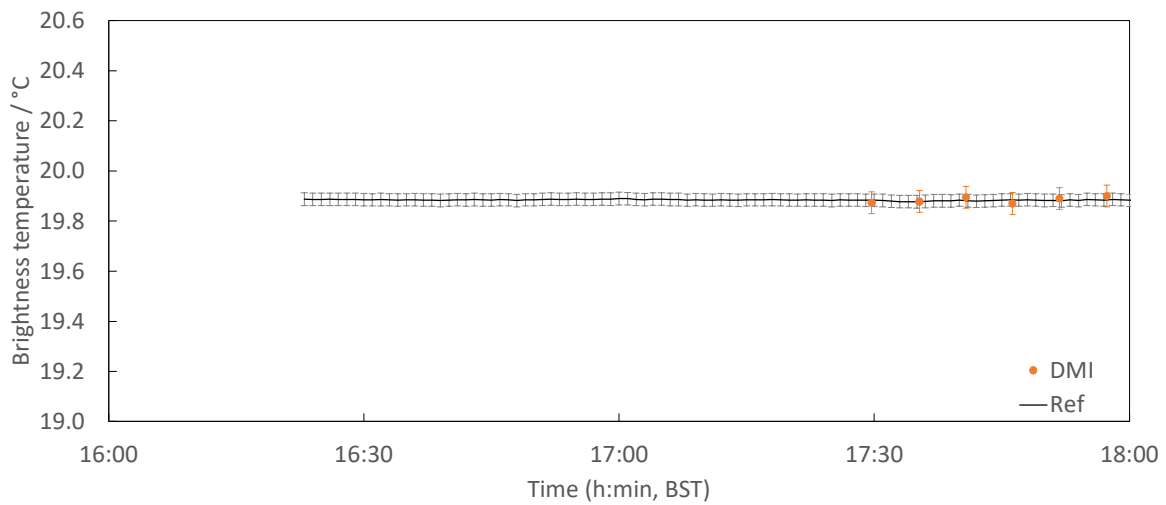
b) 20 °C (13 June 2022)

Figure 13 SL-BB measurements by DMI (Error bar denotes standard uncertainty)
(continued one next page)

c) 10 °C (14 June 2022)

d) 0 °C (15 June 2022)

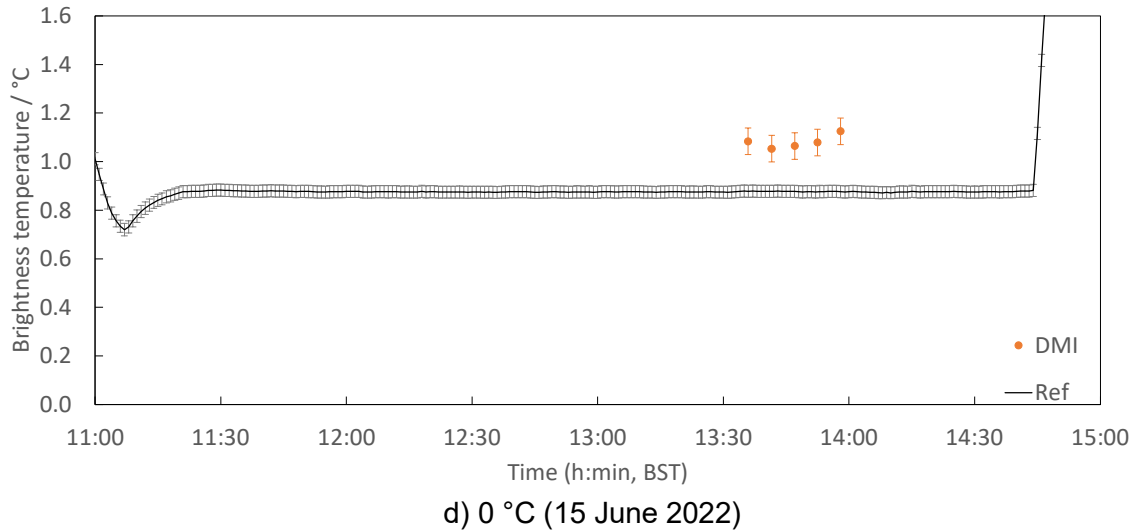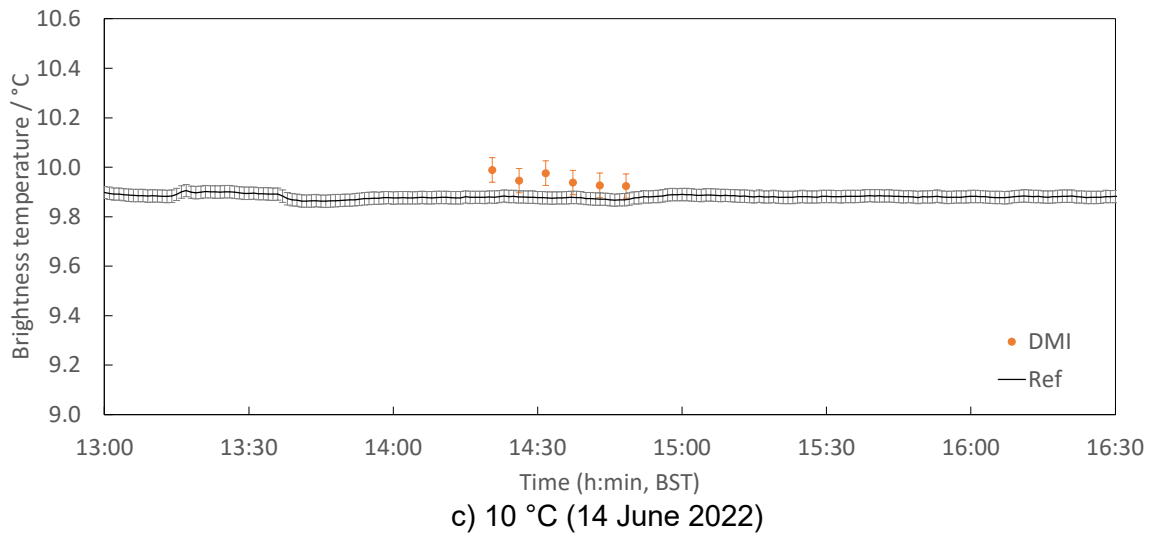Figure 13 SL-BB measurements by DMI (Error bar denotes standard uncertainty) (cont.)

a) 40 °C (16 June 2022)

Figure 14 NH3-BB measurements by DMI (Error bar denotes standard uncertainty)
(continued on next page)

b) 35 °C (13 June 2022)

c) 30 °C (14 June 2022)

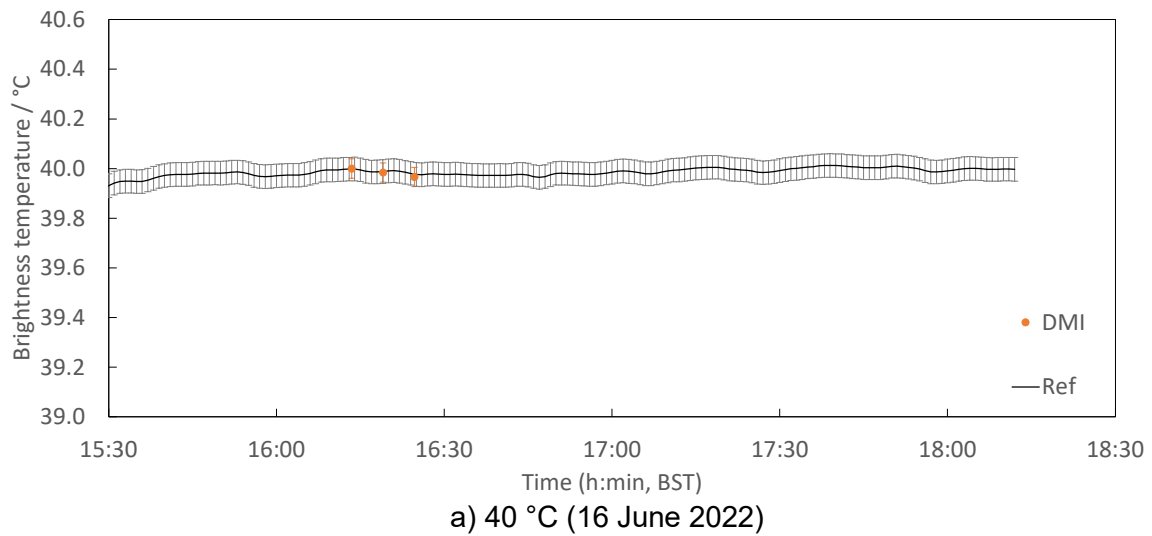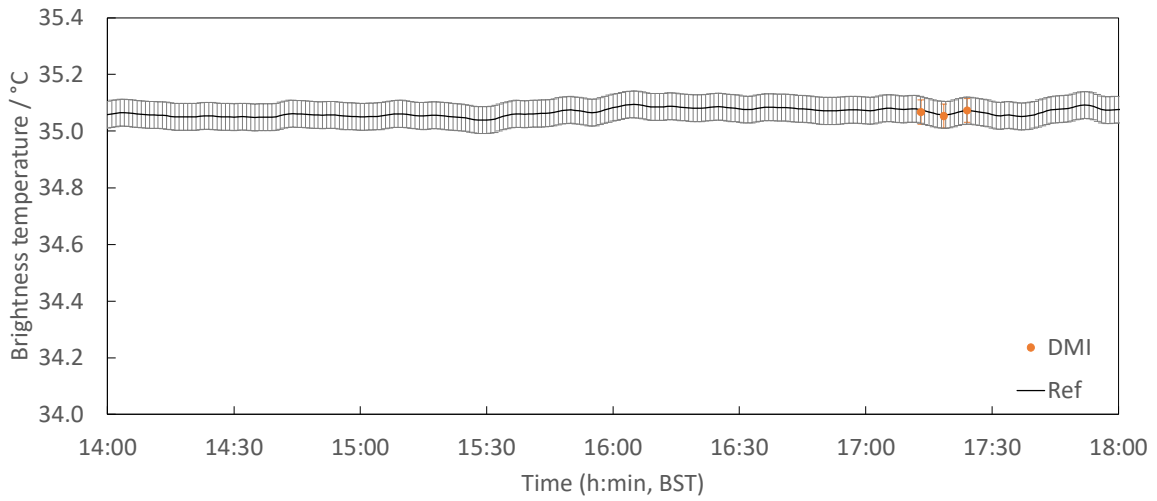
d) 0 °C (15 June 2022)

Figure 14 NH3-BB measurements by DMI (Error bar denotes standard uncertainty)
(continued on next page)

e) −15 °C (16 June 2022)
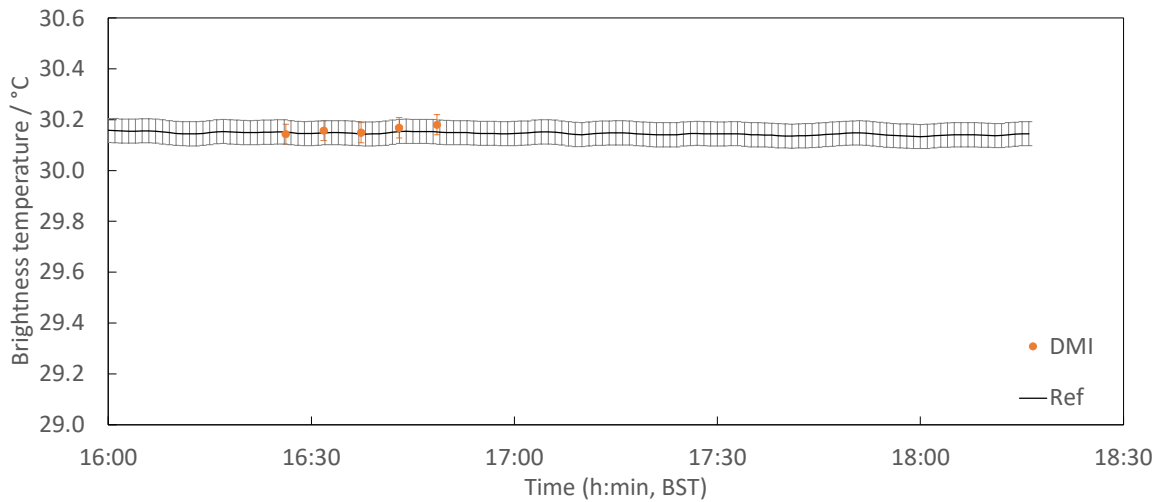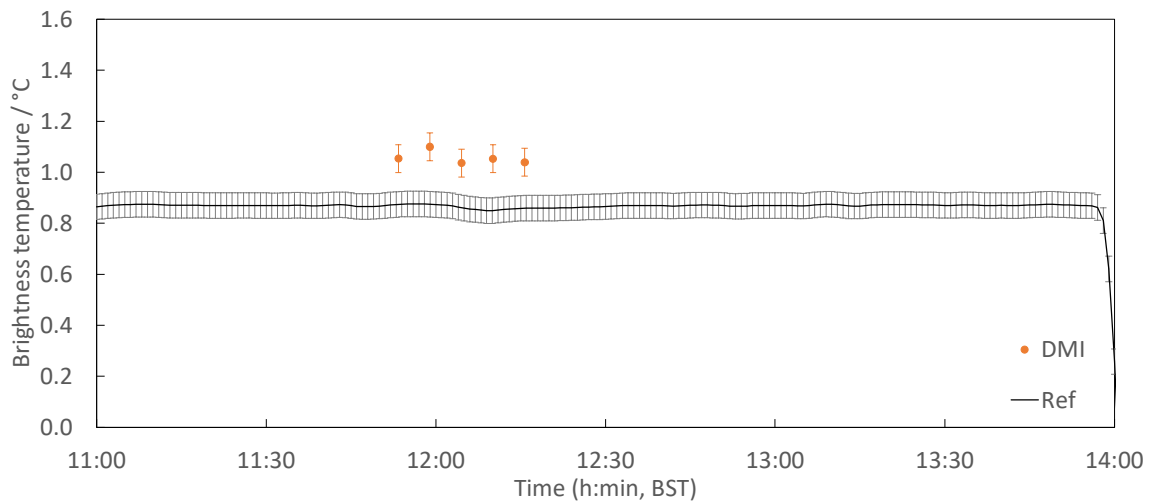
f) −30 °C (15 June 2022)
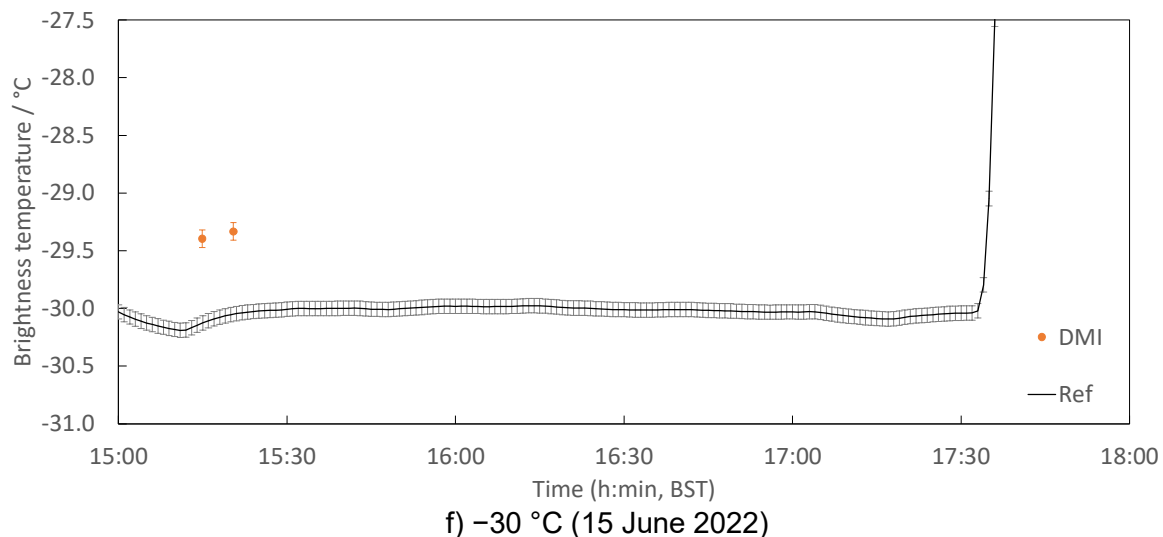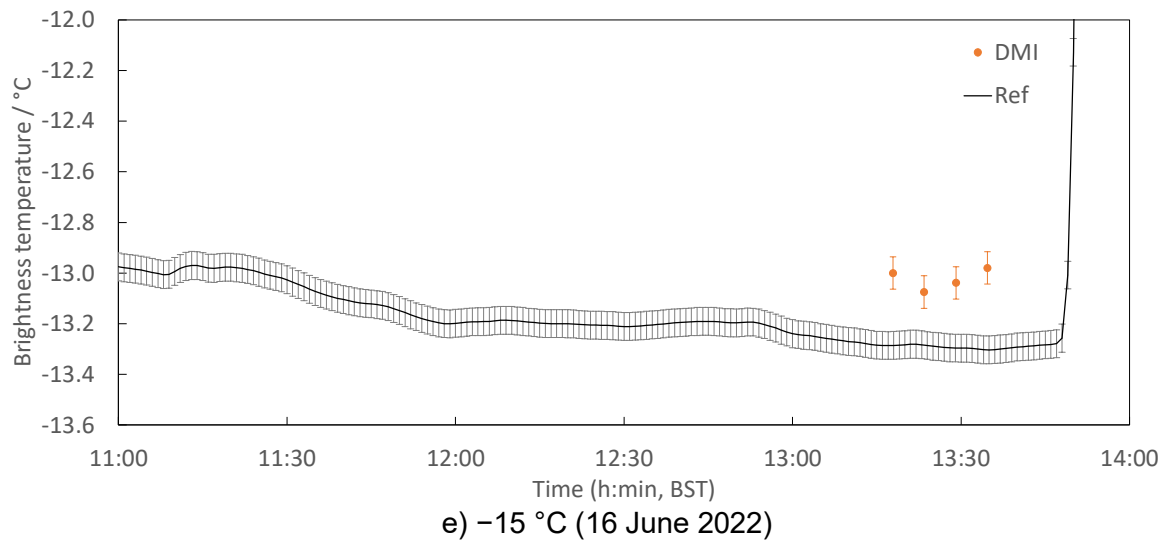
Figure 14 NH3-BB measurements by DMI (Error bar denotes standard uncertainty) (cont.)

6 OVERALL COMPARISON RESULT

6.1 TEMPERATURE DIFFERENCE FROM THE REFERENCE

The temperature differences from the reference value are plotted in Fig. 15 a) and b), for the SL-BB and the NH3-BB respectively. The temperature difference for each data plot from the reference radiance temperature at the same timing is evaluated, and the mean of the difference is evaluated.

For all of the following, different bands for the UoV CIMEL radiometers are treated as separate instruments. However, it should be noted that correlation should be expected for the uncertainty related to the calibrations, such as for offsets, if any, in the temperature of the calibration BB source.
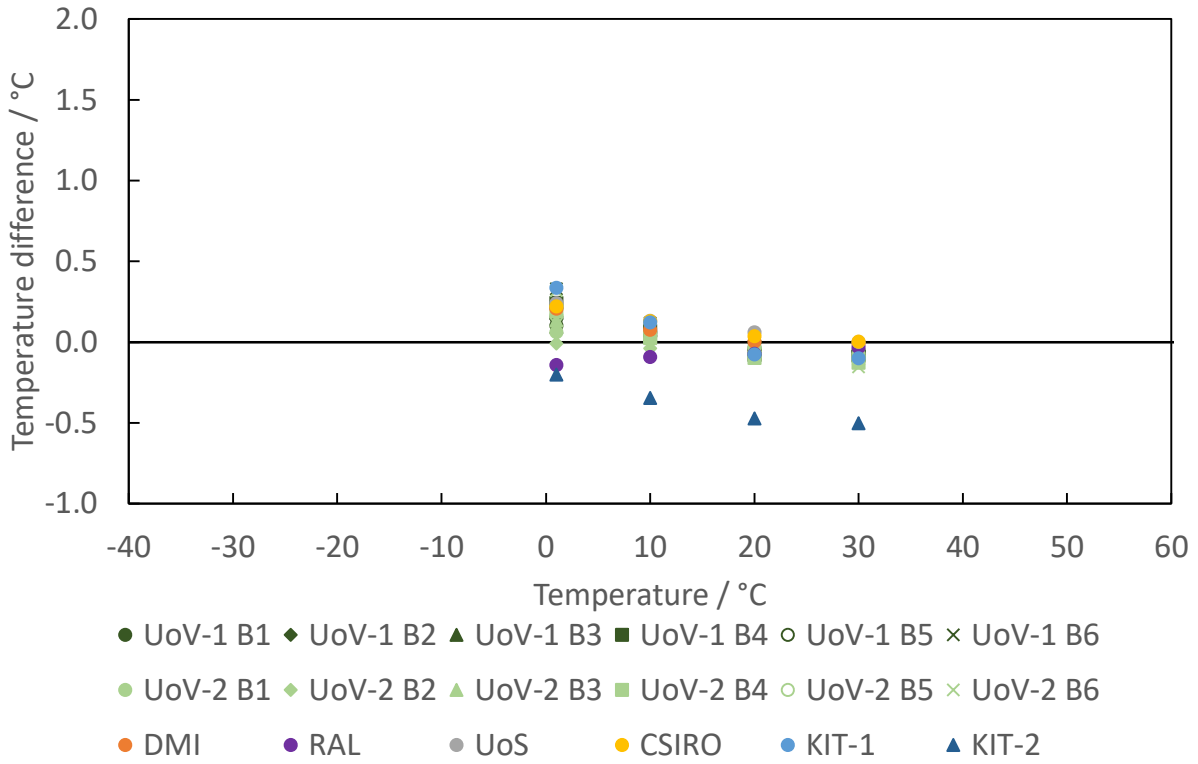
a) SL-BB
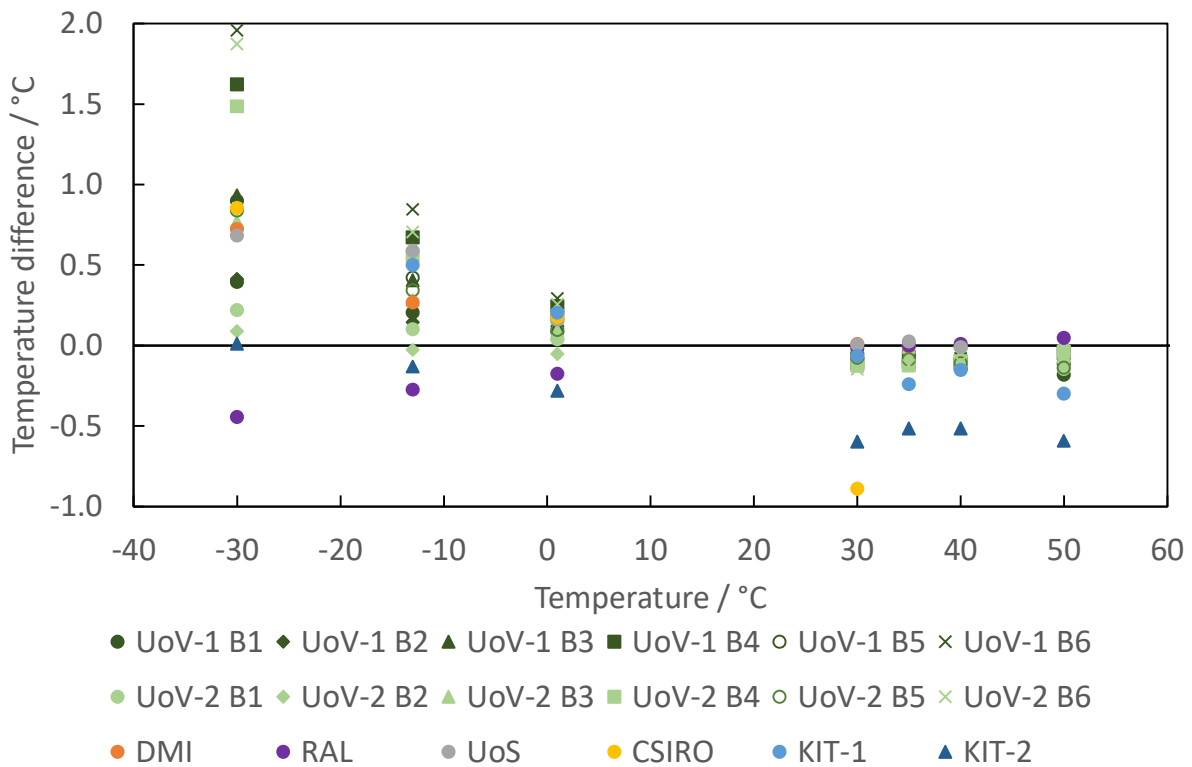
b) NH3-BB

Figure 15 Temperature differences from the reference value

6.2   AGREEMENT WITH THE REFERENCE

Agreement with the reference value is evaluated by plotting the data shown in Fig. 15 with error bars added to both the measured values and the reference value, as shown in Figs. 16 a) to e). The error bars are the expanded uncertainties ($k = 2$). At each temperature point, each participant reported either a set of time stamped measurements or a single averaged value. For the former, evaluation of the standard error of the mean of the temperature difference from the reference was evaluated for each set of measurements, and this was combined with the participant claimed combined uncertainty.

Since the ISAR and SISTeR radiometers have an internal reference blackbody to improve the accuracy of measurement, the quoted uncertainties are significantly smaller than the other two types of radiometer. Therefore, Figs. 16 a), c) and d) show results for these two instruments, while Figs. 16 b) and e) show those for the others. Note the difference in the vertical scales.
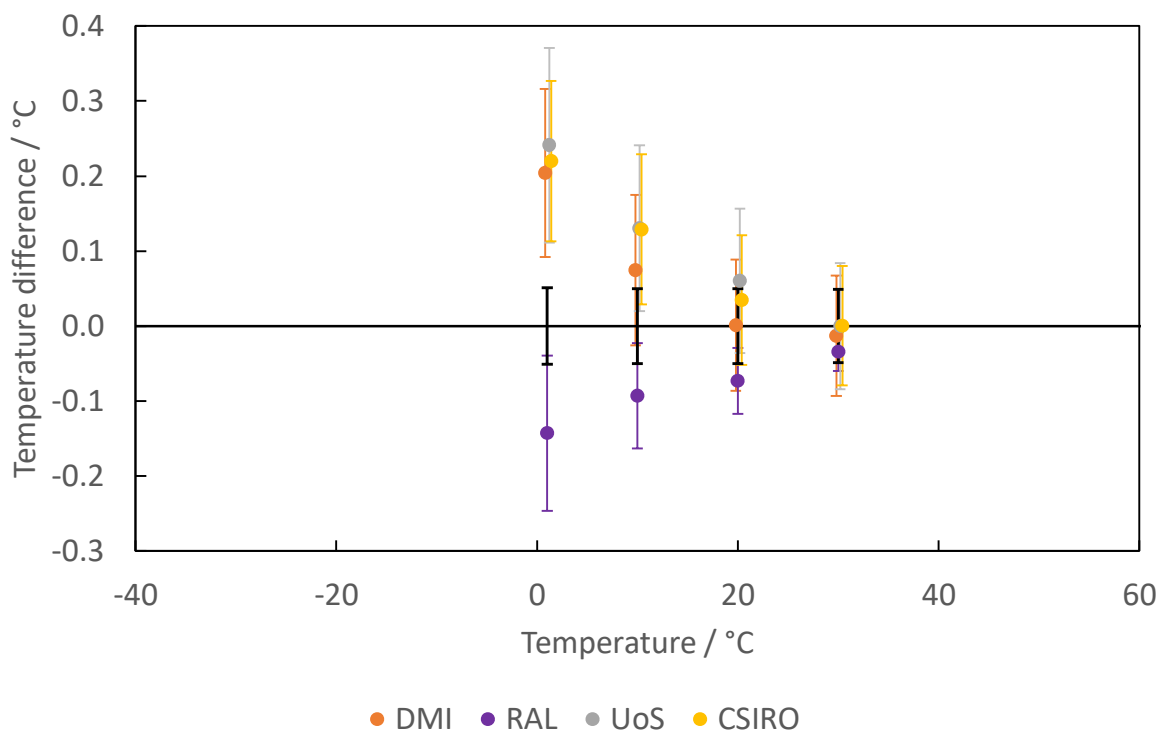
a) SL-BB measured with ISARs and SISTeR radiometers
Figure 16   Agreement with the reference value (continued on next page)
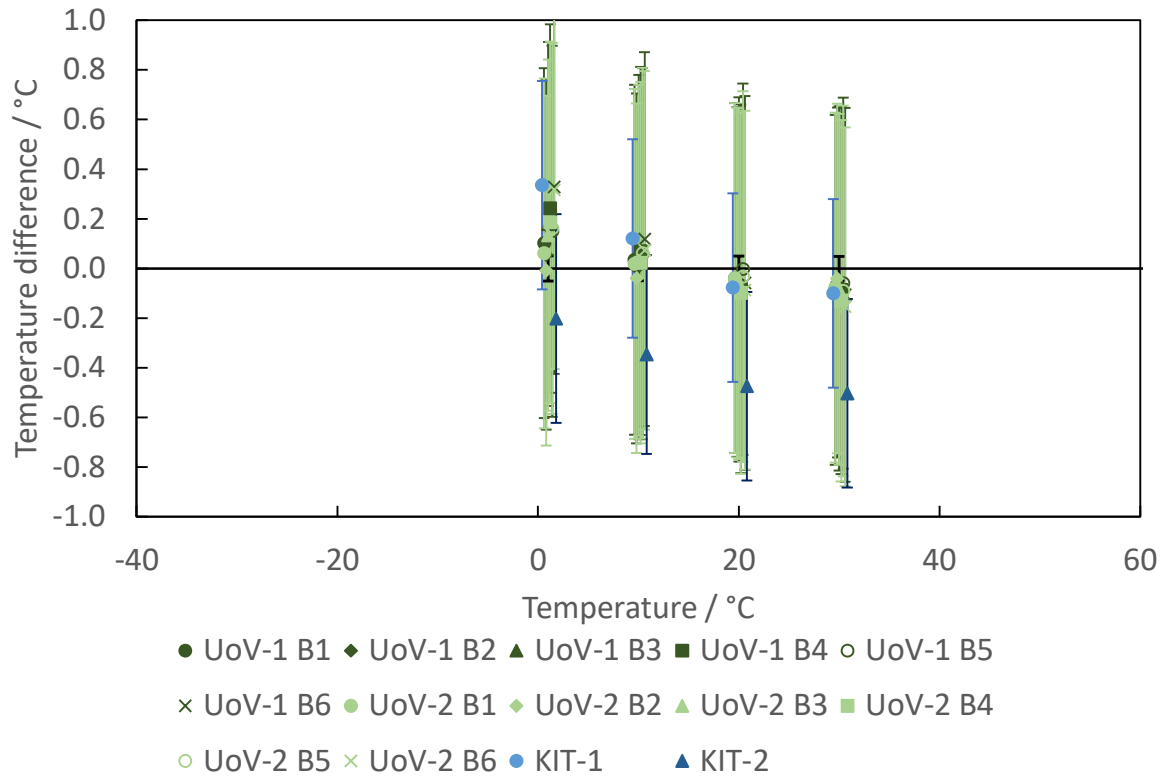
b) SL-BB measured with CIMEL and Heitronics radiometers
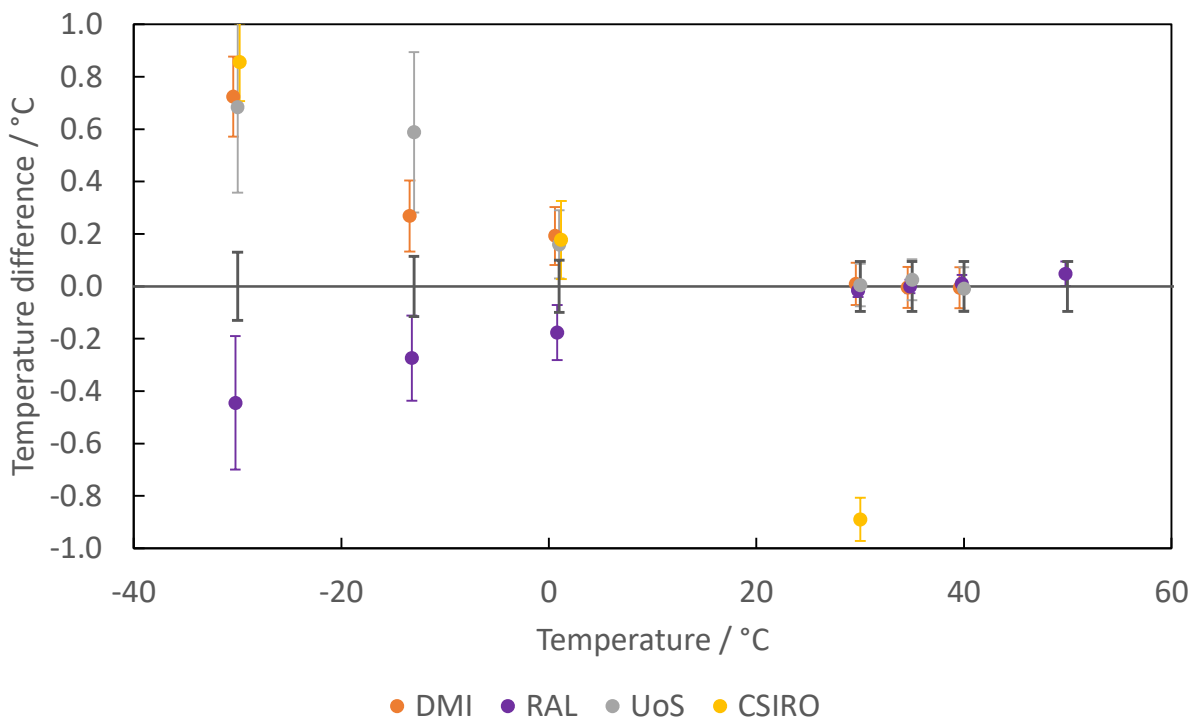
c) NH3-BB measured with ISARs and SISTeR radiometers
Figure 16 Agreement with the reference value (continued on next page)
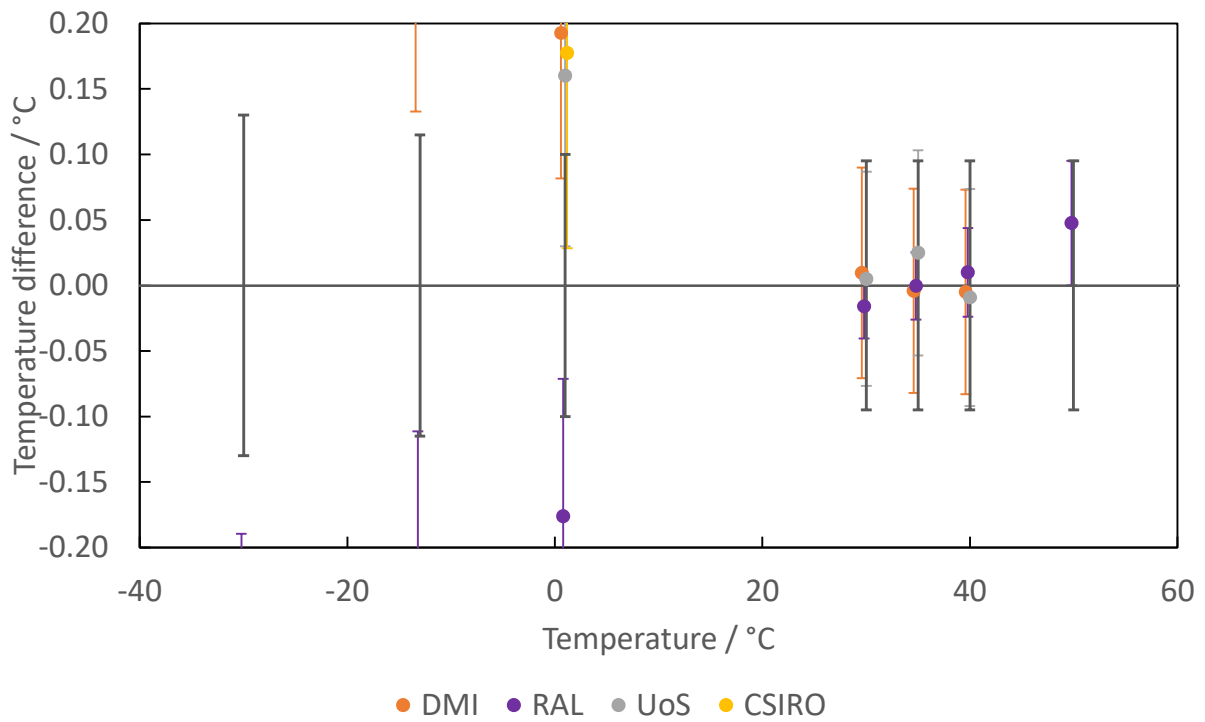
d) NH3-BB measured with ISARs and SISTeR radiometers (magnified vertical scale)
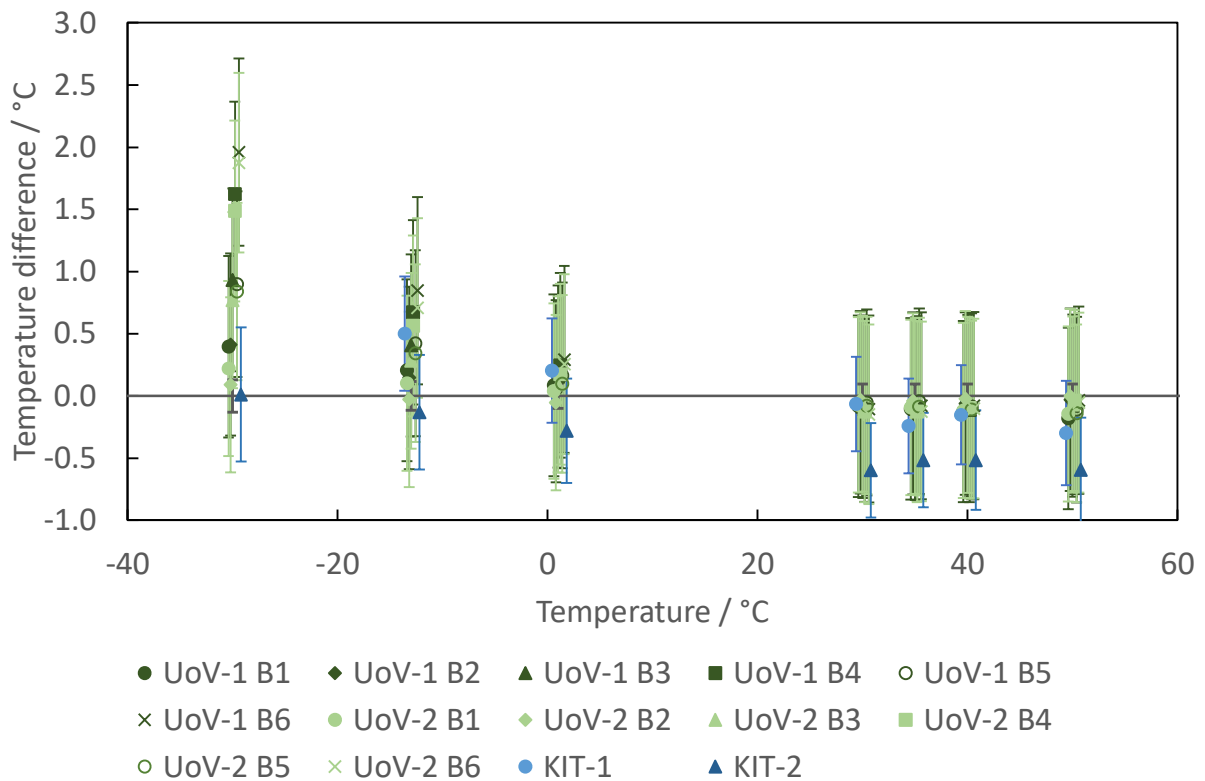
e) NH3-BB measured with CIMEL and Heitronics radiometers

Figure 16 Agreement with the reference value (cont.)
Error bars are the expanded uncertainties (*k* = 2) for the participant measured values and for the reference value. Plots are shifted slightly to make them distinguishable.

7   DISCUSSIONS

Figures 2 to 9 and 11 to 13 show that the stabilities of the reference BBs were sufficient to evaluate the agreement of the participants' scales with the SI. The evaluated standard errors of the mean for each set of measurements were all small enough that including these only increases the combined uncertainty by less than 5 %. Exceptions were some cases at −15 °C and −30 °C, and for these extreme cases, it is clear from the plots that the poor repeatability was caused by the radiometer and not the reference blackbody. For the temperature range from 0 °C to 30 °C, which is of most interest from the sea surface temperature measurement objective, the exceptional stability of the SL-BB is noticeable, and the introduction of this additional reference source for this comparison has made a positive impact.

In Fig. 15 a) and b), differences from the reference value are plotted separately for the two sources, the NH3-BB and the SL-BB. A similar trend is seen for both: good agreement around ambient temperature, and increasing difference as the temperature goes low. At 0 °C and 30 °C both sources are measured, and it can be verified that the two sources are practically equivalent. The single outlier at these two temperatures is the measurement by CSIRO of the NH3-BB at 30 °C, which shows almost 1 °C lower value than the SL-BB. This is most likely caused by an issue with the alignment of the radiometer against the NH3-BB aperture, the wide field of view of the radiometer not being fully contained within the aperture that is located deep inside from the blackbody front face (c.f. Table 3).

In the same figure, it can be seen that the scatter of the plots increases as the temperature becomes lower. This is natural since the detected radiance signal of the radiometers become low and signal-to-noise ratio decreases. Furthermore, all radiometers have some kind of an internal temperature reference kept at around ambient temperature, and therefore have the highest accuracy around this temperature. The further away the target temperature becomes from ambient, the larger the extrapolation from the internal reference, and larger the uncertainty. Finally, the BBs used to calibrate the radiometers are either a Landcal P80P or a CASOTS/CASOTS II, and in both cases they are not equipped with purge systems to prevent formation of dew and frost in the blackbody cavity. This means the use of the BBs is limited to above the dew point, which is normally above 0 °C; or, if they are used below the dew point, they could be affected by dew and frost. The participant scales are therefore most likely realized by extrapolation in the temperature ranges to below 0 °C, leading to increased uncertainty at these temperatures.

From the point of view of sea surface temperature measurement this is not an issue, since the measurement at these low temperatures are required only for measurement of the sky brightness temperature and not for the sea surface brightness temperature. Sky brightness temperature measurement error of 10 K at −30 °C will only introduce an error of around 50 mK in the measured SST, so the requirement for accuracy in the sky brightness temperature is much more relaxed.

In Fig. 16 a) to e), the agreement with the reference value is further evaluated. The expanded uncertainties ($k = 2$) are expressed by error bars for both the participant measurements and for the reference. Overlap of the error bars for the measurement and the reference, indicating the agreement of the two, is confirmed for all participants in the range 10 °C to 30 °C, which is the temperature range of interest for SST measurement. The main source of the uncertainty for the UoV and KIT radiometers corresponds to the primary calibration uncertainty (from the Landcal P80P BB used), which is 0.34 K for UoV and 0.15 K for KIT ($k = 1$, see sections 5.1.1 and 5.2.1). However, the good agreement in the current comparison result indicates this is likely an overestimation. This is further confirmed in the accompanying blackbody comparison [AD-4]. Investigation is envisaged to determine a more realistic reduced calibration uncertainty.

In Fig. 16, separate graphs are shown for the NH3-BB and the SL-BB. Also the ISAR and SISTeR radiometers, which have smaller uncertainties, are plotted separately from the other instruments with larger uncertainties. It is clear from the graphs that all three ISARs agree very well each other while the SISTeR shows a different trend. A systematic error in the ISAR instrument may be present. An investigation into the cause is recommended for improved reliability.

In the temperature range below 0 °C the error bars of the measurements do not necessarily overlap with that of the reference, indicating that the uncertainty estimation does not fully represent the true measurement capabilities of the participants. As described above, lower temperature introduces various difficulties for accurate temperature measurements, but the declared uncertainties do not increase as expected, and for some participants they are almost the same as in the ambient temperature range. Without reliable uncertainty values assigned, the measured values themselves lack reliability. Even though high accuracy is not a requirement for sky brightness temperature, investigation is desirable for all participants to ensure the uncertainties reflect the true capabilities.

Figure 17 Comparison participants

8 CONCLUSIONS

Six radiometers for sea surface temperature measurement were compared against the NPL reference standard BBs as a part of the CEOS International Thermal Infrared Radiometer Inter-comparison (CRIC). During the comparison, which took place during five days in June 2022, the six radiometers viewed the cavities of an NH3-BB and a SL-BB, and radiance temperatures detected by the radiometers were compared against the values derived from the platinum resistance thermometers measuring the BBs, which were calibrated traceable to the ITS-90 primary standards of NPL.

Introducing the new SL-BB to the comparison proved to have a positive impact, not only for improved efficiency of the measurements, but also from the point of view of improvement in measurement accuracy by the participants owing to its large aperture, high emissivity, and temporal stability. Measurement of the two BBs made at same temperatures showed similar agreement, which confirmed that they produce identical comparison results.

The SL-BB was applied for comparison in the range 0 °C to 30 °C. The temperature range of most interest from the SST measurement point of view is 10 °C to 30 °C, and in this temperature range all participants reported results that were in agreement with the reference.

The NH3-BB was applied to the extreme temperatures at -30 °C, -15 °C, 0 °C, 30 °C, 35 °C, 40 °C, and 50 °C. The temperatures above 30 °C showed good agreement, similar to 30 °C. On the other hand, at and below 0 °C, the participant reported values showed divergence from the reference which grew as the temperature became lower, and the divergence exceeded the uncertainties. This will not have a major significance in the SST measurement, since this low temperature range is only required for sky brightness temperature measurement, which will only be used for correction of the reflection at sea surface that requires low accuracy. However, it indicates there is deficiency in the uncertainty estimation capability in all participants, especially when the measured sea surface temperature deviates from the ambient, and this should be improved in future if the participants are to maintain confidence in their SST measurement capabilities.

It should also be noted that the comparison in the laboratory is not always equivalent to measurement in the field. The comparison results show that divergence from the reference is noticeable where the target temperature diverts from the ambient temperature. The instruments tested here utilise internal reference BBs at temperatures at around the ambient, which means high accuracy is expected if the target is around the ambient. In the laboratory, this is not always the case, for the room temperature is maintained around 23 °C regardless of the blackbody source temperature. On the other hand, in the field the ambient temperature is always close to the SST. Performance of the instruments when measuring SST should therefore be expected to be better in practice compared to what this comparison shows, and the results shown in this comparison should be interpreted as a worst case scenario. The result of the field comparison shows very good agreement among participants, and this seems to support the above observation [AD-5].

A group photograph of the participants is shown in Fig.17. It was unfortunate that the number of participants was smaller than the last comparison primarily due to travel restrictions imposed by the COVID-19 pandemic. In recent years, new improved radiometers for SST measurements are being developed, and more radiometers are being deployed at the sea. A future repeat of the current exercise will be needed, possibly with a reduced interval between comparisons than the current six to eight years, when the new radiometers are being used in the field.

References

[1] Barton, I. J., Minnett, P. J., Maillet K. A., Donlon, C. J., Hook, S. J., Jessup, A. T. and Nightingale, T.J. (2004) "The Miami 2001 infrared radiometer calibration and intercomparison: Part II Shipboard results", *J. Atmos. Ocean Techn.,* 21, 268-283.

[2] Rice, J. P., Butler, J. I., Johnson, B. C., Minnett, P. J., Maillet K. A., Nightingale, T. J, Hook, S. J., Abtahi, A., Donlon, and. Barton, I. J. (2004) "The Miami 2001 infrared radiometer calibration and intercomparison. Part I: Laboratory characterisation of blackbody targets", *J. Atmos. Ocean Techn.,* 21, 258-267.

[3] Theocharous, E. and Fox, N. P. (2010) "CEOS comparison of IR brightness temperature measurements in support of satellite validation. Part II: Laboratory comparison of the brightness temperature of blackbodies", *NPL Report COM OP4*.

[4] Theocharous, E., Usadi, E. and Fox, N. P. (2010) "CEOS comparison of IR brightness temperature measurements in support of satellite validation. Part I: Laboratory and ocean surface temperature comparison of radiation thermometers", *NPL Report COM OP3*.

[5] Theocharous, E., Barker Snook, I. and Fox, N. P. (2017) "2016 comparison of IR brightness temperature measurements in support of satellite validation. Part 1: Laboratory comparison of the brightness temperature of blackbodies", *NPL Report ENV 12*.

[6] Theocharous, E., Barker Snook, I. and Fox, N. P. (2017) "2016 comparison of IR brightness temperature measurements in support of satellite validation. Part 2: Laboratory comparison of radiation thermometers", *NPL Report ENV 14*.

[7] Theocharous, E., Barker Snook, I. and Fox, N. P. (2017) "2016 comparison of IR brightness temperature measurements in support of satellite validation. Part 3: Sea surface temperature comparison of radiation thermometers", *NPL Report ENV 15*.

[8] Theocharous, E., Fox, N. P., Barker-Snook, I., Niclòs, R., García-Santos, V., Minnett, P. J., Göttsche, F. M., Poutier, L., Morgan, N., Nightingale, T., Wimmer, W., Høyer, J., Zhang, K., Yang, M., Guan, L., Arbelo, M. and Donlon, C. J. (2019) "The 2016 CEOS infrared radiometer comparison: Part 2: Laboratory comparison of radiation thermometers", *J. Atmos. Ocean Techn.,* 36, 1079-1092.

[9] https://www.bipm.org/documents/20126/41791796/ITS-90.pdf

[10] Chu, B. and Machin, G. (1999) "A low-temperature blackbody reference source to −40 °C", *Meas. Sci. Technol.* 10, 1-6.

[11] Simpson, R., et al., (in preparation)

[12] Sicard, M., Spyak, P. R., Brogniez, G., Legrand, M., Abuhassan, N. K., Pietras, C., and Buis, J. P. (1999). "Thermal infrared field radiometer for vicarious cross-calibration: characterization and comparisons with other field instruments", *Optical Engineering*, 38 (2), 345-356.

[13] Legrand, M., Pietras, C., Brogniez, G., Haeffelin, M., Abuhassan, N. K. and Sicard, M. (2000). "A high-accuracy multiwavelength radiometer for in situ measurements in the thermal infrared. Part I: characterization of the instrument", *J. Atmos. Ocean Techn.,* 17, 1203-1214.

[14] Coll, C., Niclòs, R., Puchades, J., García-Santos, V., Galve, J.M., Pérez-Planells, L., Valor, E., Theocharous, E. (2019) "Laboratory calibration and field measurement of land surface temperature and emissivity using thermal infrared multiband radiometers", *Int. J. Appl. Earth Obs. Geoinformation*, 78, 227-239.

[15] Donlon, C., Robinson, I. S., Wimmer, W., Fisher, G., Reynolds, M., Edwards, R., & Nightingale, T. J. (2008) "An infrared sea surface temperature autonomous radiometer (ISAR) for deployment aboard volunteer observing ships (VOS)". *J. Atmos. Ocean Techn.,* 25, 93-113.

[16] Wimmer, W., and Robinson, I. (2016) "The ISAR instrument uncertainty model", *J. Atmos. Ocean Techn.,* 33, 2415-2433

[17] Donlon, C., Wimmer, W., Robinson, I. S., Fisher, G., Ferlet, M., Nightingale, T. J. and Bras, B. (2014) "A Second-Generation Blackbody System for the Calibration and Verification of Seagoing Infrared Radiometers", *J. Atmos. Ocean Techn.,* 31, 1104-1127

[18] https://webarchive.nationalarchives.gov.uk/ukgwa/20210603104457/https://stfc.ukri.org/research/environment/sister/